

Oxygen isotope systematics of chondrules in the Allende CV3 chondrite: High precision ion microprobe studies

N. G. Rudraswami*†, T. Ushikubo, D. Nakashima, and N. T. Kita

WiscSIMS, Department of Geoscience, University of Wisconsin-Madison
1215 W. Dayton, Madison WI 53706, USA.

†Present Address: National Institute of Oceanography, Council of Scientific and Industrial
Research, Dona Paula - 403 004, Goa, India

*Corresponding author: rudra@nio.org

Abstract: The oxygen three-isotope systematics of 36 chondrules from the Allende CV3 chondrite are reported using high precision secondary ion mass spectrometer (Cameca IMS-1280). Twenty-six chondrules have shown internally homogenous $\Delta^{17}\text{O}$ values among olivine, pyroxene, and spinel within a single chondrule. The average $\Delta^{17}\text{O}$ values of 19 FeO-poor chondrules (13 porphyritic chondrules, 2 barred olivine chondrules, and 4 chondrule fragments) show a peak at $-5.3 \pm 0.6\text{‰}$ (2SD). Another 5 porphyritic chondrules including both FeO-poor and FeO-rich ones show average $\Delta^{17}\text{O}$ values between -3‰ and -2‰ , and 2 other FeO-poor barred olivine chondrules show average $\Delta^{17}\text{O}$ values of -3.6‰ and 0‰ . These results are similar to those for Acfer 094 chondrules, showing bimodal $\Delta^{17}\text{O}$ values at -5‰ and -2‰ . Nine porphyritic chondrules contain olivine grains with heterogeneous $\Delta^{17}\text{O}$ values as low as -18‰ , indicating that they are relict olivine grains and some of them were derived from precursors related to refractory inclusions. However, most relict olivine grains show oxygen isotope ratios that overlap with those in homogeneous chondrules. The $\Delta^{17}\text{O}$ values of four barred olivine chondrules range from -5‰ to 0‰ , indicating that not all BO chondrules plot near the Terrestrial Fractionation line as suggested by previous bulk chondrule analyses. Based on these data, we suggest the presence of multiple oxygen isotope reservoirs in local dust-rich protoplanetary disk, from which the CV3 parent asteroid formed.

A compilation of 225 olivine and low-Ca pyroxene isotopic data from 36 chondrules analyzed in the present study lie between CCAM (carbonaceous chondrite anhydrous mineral) and Young and Russell lines. These data define a correlation line of $\delta^{17}\text{O} = (0.982 \pm 0.019) \times \delta^{18}\text{O} - (2.91 \pm 0.10)$, which is similar to those defined by chondrules in CV3 chondrites and Acfer 094 in previous studies. Plagioclase analyses in two chondrules plot slightly below the CCAM line with $\Delta^{17}\text{O}$ values of -2.6‰ , which might be the result of oxygen isotope exchange between chondrule mesostasis and aqueous fluid in the CV parent body.

1. INTRODUCTION

Early solar system objects have shown diversity in oxygen isotope reservoirs suggesting isotopic heterogeneity in the solar nebula (Clayton et al., 1993). The large variation ($\geq 50\text{‰}$) of oxygen three isotopes in Calcium Aluminium rich inclusions (CAIs) lie along a slope of ~ 1 on $\delta^{18}\text{O}$ versus $\delta^{17}\text{O}$ graph, and this is commonly referred to as the carbonaceous chondrite anhydrous mineral (CCAM; Clayton et al., 1973, 1977) line. This line is distinct from the terrestrial mass fractionation (TF) line, which has a slope of ~ 0.5 . Solid components in the early solar system might acquire ^{16}O -depleted oxygen isotope ratios through processes involving mass independent fractionation of oxygen isotopes (e.g., Thiemens and Heidenreich, 1983; Yurimoto and Kuramoto, 2004; Lyons and Young, 2005). The oxygen isotope ratios in chondrules, which formed at least 2 Ma after the formation of CAIs (e.g., Kita et al., 2000; Rudraswami and Goswami, 2007; Rudraswami et al., 2008; Kurahashi et al., 2008), are generally depleted in ^{16}O compared to CAIs (Krot et al., 2006, references therein).

A number of bulk oxygen isotope analyses of chondrules in Allende and other CV3 chondrites have been reported and they plot near and along the CCAM line at the ^{16}O poor end with significant variations (Rubin et al., 1990; Clayton et al., 1993; Jabeen et al., 1998a, 1998b; Young et al., 2002; Jones et al., 2004). Jones et al. (2004) performed oxygen three-isotope analyses of chondrules in the Mokoia CV3 carbonaceous chondrite using both bulk laser fluorination gas mass spectrometer and in-situ secondary ion mass spectrometer (SIMS, or ion microprobe). They found that the ion microprobe analyses of olivine in chondrules show more enrichment in ^{16}O than bulk analyses of the same chondrules. Internal heterogeneity of oxygen isotope ratios among olivine, pyroxene, and mesostasis in chondrules were obtained using ion microprobe from CV3 and CR2 chondrites (Maruyama et al., 1999; Maruyama and Yurimoto, 2003; Chaussidon et al., 2008). The partial oxygen isotope exchange between solid precursor material and nebular gas may be responsible for significant oxygen isotopic zonation within a single porphyritic chondrule (e.g., Yu et al., 1995). Barred olivine (BO) chondrules measured by Clayton et al. (1983) fall close to the TF line in a three oxygen isotope plot, which was interpreted as reflecting isotope ratios in nebular gas by complete melting of the chondrule (hence, the BO texture). Chaussidon et al. (2008) independently estimated similar oxygen isotope ratios of the solar nebula according to the oxygen isotope zoning of chondrules between olivine and pyroxene. They further speculated that olivine grains in FeO-poor (type I) porphyritic chondrules originated from a differentiated planetesimal that existed prior to chondrule formation processes (Libourel and Krot, 2007).

Recently, Ushikubo et al. (2009, 2011) performed high precision oxygen three-isotope analyses of ~40 chondrules in the Acfer 094 carbonaceous chondrite using an ion microprobe CAMECA IMS-1280 at the University of Wisconsin. While nearly a half of the chondrules in Acfer 094 contain relict olivine grains with a wide range of oxygen isotope ratios, with some as low as -50‰ in $\delta^{18}\text{O}$ and $\delta^{17}\text{O}$ values, olivine in these chondrules generally show indistinguishable oxygen isotope ratios relative to pyroxene, plagioclase, and/or glass in the same chondrules. Furthermore, Ushikubo et al. (2011) showed that $\Delta^{17}\text{O}$ ($= \delta^{17}\text{O} - 0.52 \times \delta^{18}\text{O}$), exhibits a bimodal distribution, i.e. one peak at -5‰ and another at -2‰ from which they concluded that chondrules in Acfer 094 formed in two distinct oxygen isotope reservoirs that existed in the local protoplanetary disk. The isotope reservoir with $\Delta^{17}\text{O} = -2‰$ is widely recognized among chondrules in carbonaceous chondrites, such as those in CR, CH, and CB (Krot et al., 2006, 2010), as well as a chondrule-like object from cometary particles recovered from the Stardust mission (Nakamura et al., 2008). Therefore, identification of common isotope reservoirs among chondrules in different classes of chondrites is very important to understand how they were distributed throughout the early solar system.

In this study, we report high precision ion microprobe oxygen isotope analyses of chondrules in the Allende CV3.2 chondrite, which is the most widely studied in terms of chondrule bulk oxygen isotopes (Clayton et al., 1983; Rubin et al., 1990). The Allende meteorite shows evidence of thermal metamorphism and aqueous alteration in its parent body (Krot et al., 1998a, 1998b); as a result, we focus mainly on analysis of olivine and low-Ca pyroxene phenocrysts, which preserve primary isotope signatures at the time of chondrule formation. The main objectives of this study are as follows:

- (1) To compare oxygen three-isotope ratios between olivine and low-Ca pyroxene within chondrules in Allende to test if the chondrule formed from a melt with homogeneous oxygen isotope ratios.
- (2) To examine the distribution of $\Delta^{17}\text{O}$ values among chondrules in Allende to determine if they show a bimodal distribution at $\Delta^{17}\text{O}$ values of -5‰ and -2‰, similar to the observation from chondrules in Acfer 094 (Ushikubo et al., 2011).

In addition, we examined several BO chondrules in order to compare our ion microprobe results to those of Clayton et al. (1983), who showed that bulk BO chondrules plot near the TF line. Three spinel bearing chondrules in Allende were also analyzed in this study, in order to test the origin of spinel in chondrules, as spinel may be relict material from refractory inclusions (e.g., Maruyama et al., 1999) or it may be co-genetic (e.g., Maruyama et al., 1999; Ma et al., 2008).

The new generation of ion microprobe at WiscSIMS laboratory is capable of obtaining oxygen three-isotope ratios from a ~ 15 μm spot with external reproducibility as good as 0.3‰ (e.g., Kita et al., 2009; Valley and Kita, 2009). This permits us to be able to distinguish relict grains within the individual chondrules if they differ in oxygen isotope ratios by more than 1‰ (Ushikubo et al., 2011). Therefore the ability to analyze individual phases in Allende CV3 chondrules by ion microprobe, as opposed to bulk analyses of Allende by other techniques, will allow us to provide enhanced important information for understanding many aspects of oxygen isotope reservoirs near the CV chondrule-forming region of the early solar nebula.

2. SAMPLES AND ANALYTICAL TECHNIQUES

2.1. Samples

The Allende meteorite is an oxidized CV3 chondrite with shock stage S1 and a petrographic grade of 3.2 (Krot et al., 1998a, 1998b). Four Allende polished sections were used in this study: two thin sections allocated from the National Museum of Natural History at the Smithsonian Institution (section numbers USNM-3658-2 and USNM-3510-8), and two thick sections from the Physical Research Laboratory at Ahmedabad. We selected 36 chondrules from more than few hundred chondrules examined in these four sections based on the criteria that they contain large (>50 μm) olivine and/or pyroxene grains for multiple analyses using 15 μm spot of ion microprobe beam, and that they cover representative types of chondrules. These chondrules may be somewhat biased towards porphyritic olivine (PO) chondrules with large olivine phenocrysts, due to selection criteria. Type II and BO chondrules were also selected, though they are under-represented. We did not select radial pyroxene and cryptocrystalline chondrules for oxygen isotope studies due to the small sizes of individual crystals.

2.2. Electron microscopy

A Hitachi S3400 variable pressure scanning electron microscope (SEM) at the University of Wisconsin was used for observing the meteorite samples. The four sections of the Allende meteorite were initially documented using the SEM with back scattered electron (BSE) and secondary electron (SE) imaging that provides high resolution images suitable for identifying microscopic individual phases of olivine, pyroxene, spinel and plagioclase within chondrules. The energy dispersive X-ray (EDX) detector was also used for initial identification of different minerals in the chondrules. Major element compositions (Na_2O , MgO , Al_2O_3 , SiO_2 , CaO , TiO_2 , Cr_2O_3 , MnO and FeO) of minerals were obtained using a Cameca SX-51 electron probe micro-analyzer (EPMA, or electron

microprobe) at the University of Wisconsin. The instrument parameters used for electron microprobe are: acceleration voltage of 15 kV, a beam current of 12 nA and a beam diameter of 1–2 μm using wavelength dispersive X-ray spectroscopy. Data reduction and corrections were performed with probe for windows software. We typically obtained ~25 electron microprobe data points of phases of interest from each chondrule, and used the location of electron microprobe analyses as a guide when performing ion microprobe analysis. This selection covers different mineral phases and wide range of major element compositions.

2.3. Ion microprobe analyses of oxygen three isotopes

The oxygen three-isotope analyses of Allende chondrules were made using a large radius (=585 mm) ion microprobe, CAMECA IMS-1280 at the University of Wisconsin (WiscSIMS). A detailed description of the analytical method is reported elsewhere (Kita et al., 2009, 2010; Heck et al., 2010). We used a focused Cs^+ primary beam with a current of 3–4 nA and a spot size of ~15 μm on the sample surface, and secondary oxygen ions ($^{16}\text{O}^-$, $^{17}\text{O}^-$ and $^{18}\text{O}^-$) were detected using multi-collection Faraday cup (FC) detectors. The intensity of $^{16}\text{O}^-$ was $(3\text{--}4) \times 10^9$ cps (counts/second). The peak height of OH^- interference was examined after each analysis to estimate the tailing contribution of OH^- peak to the $^{17}\text{O}^-$ peak, which was found to be negligibly small in all cases (<0.1%). The oxygen isotope ratios of $^{17}\text{O}/^{16}\text{O}$ and $^{18}\text{O}/^{16}\text{O}$ are expressed in δ -notation, as $\delta^{17}\text{O}$ and $\delta^{18}\text{O}$, respectively, which are deviation in parts per thousand from those in Standard Mean Ocean Water (SMOW). The deviation of oxygen three-isotope ratios from the terrestrial mass fractionation line is represented by $\Delta^{17}\text{O} = \delta^{17}\text{O} - 0.52 \times \delta^{18}\text{O}$ (Clayton et al., 1993).

A thin section of San Carlos olivine standard was used as the running standard for correcting the instrumental bias. The 15–20 analyses on chondrule mineral phases are bracketed by 8–10 standard analyses of San Carlos olivine ($\delta^{18}\text{O} = 5.32 \pm 0.08\text{‰}$; Kita et al., 2010). The external errors of individual analyses, or spot-to-spot reproducibility, are estimated from the 2 standard deviation (2SD) of 8 bracketing standard analyses, which are typically 0.3‰ for all ratios. Instrumental biases for other minerals were estimated from analyses of suites of terrestrial pyroxene, plagioclase and spinel standards within the same analytical session (e.g., Valley and Kita, 2009; Kita et al., 2010). For oxygen isotope measurements of pyroxene and plagioclase in chondrule, instrumental bias is corrected as a function of their wollastonite (Wo%) and anorthite (An%) contents, respectively, from electron microprobe analyses (Kita et al., 2010).

After oxygen isotope analyses, each spot was re-examined with SEM to confirm its position of analysis and its pit shape. Additionally we checked for unknown cracks, grain boundaries and/or

inclusions within ion microprobe pits, which are often correlated with erroneous obtained oxygen isotope ratios. This methodology helped us to get rid of the strange oxygen isotope data from irregular analysis pits.

3. RESULTS

Mineralogy, type of chondrules and major element composition of minerals (olivine, pyroxene, spinel and plagioclase) are listed in [Table 1](#). Among the 31 type I (FeO-poor, Mg# (= molar $[\text{MgO}]/[\text{MgO}+\text{FeO}]\%$) ≥ 90) chondrules, 22 show porphyritic textures, i.e. 15 porphyritic olivine chondrules (PO; modal abundance of olivine $>80\%$ and also referred to as IA), 6 porphyritic olivine-pyroxene chondrules (POP; modal abundance of olivine 20–80%; IAB), and 1 porphyritic pyroxene chondrule (PP; modal abundance of olivine $<20\%$; IB). The rest of the type I chondrules are: 1 plagioclase rich (PR) chondrule, 4 barred olivine (BO) chondrules, and 4 chondrules fragments that contain large forsteritic olivine phenocrysts. The texture of these type I chondrule fragments (hereafter refer as “IF”) are not easily recognized, though they may be either type IA or type IAB porphyritic chondrules. Five type II (FeO-rich, Mg# <90) chondrules are all porphyritic chondrules and comprise of 4 PO (IIA) and 1 POP (IIAB). Representative BSE images for different chondrule types from Allende are given in [Fig. 1](#) and BSE images of all chondrules analyzed for oxygen three isotopes are given in [EA1](#). Representative electron microprobe analyses of individual minerals in each chondrule are shown in [EA2](#). The type I chondrules are widely present and range in size from 500–1200 μm , while type II chondrules are less abundant and are generally smaller in size (~ 300 –700 μm). In many cases, the Mg# of olivine is slightly lower than those in low-Ca pyroxene ([Table 1](#)) within the same chondrule, which may be caused by Mg-Fe exchange in the parent body due to mild thermal metamorphism (Krot et al., 1995). Some chondrules show petrologic evidence of relict olivine grains, such as dusty olivine grains in type I chondrules (ALL-2-CH-25; [Fig. 1a](#)) and forsteritic olivine in type II chondrules (ALL-1-CH-32 and 3510-CH-43; [Figs. 1e and f](#)), which is described in the subsection 3.1.2.

In each chondrule six to eight spots were chosen for ion microprobe analysis of different minerals depending on the grain size and surface features. The majority of minerals analyzed were olivine and low-Ca pyroxene. In addition, high-Ca pyroxene, spinel and plagioclase grains were also analyzed, when grain size exceeded 20 μm . The total numbers of oxygen three-isotope analyses (individual spot) were 184 for olivine, 38 for low-Ca pyroxene, 4 for high-Ca pyroxene, 8 for spinel, and 6 for plagioclase. The full data set of oxygen three-isotope analyses for the 36 chondrules is given in [EA3](#). All the errors reported for the individual spot analyses in [EA3](#) are 2SD of bracketing

standard that represent external error. The spots analyzed in each chondrule are marked in the BSE images in EA1 according to the number given in oxygen isotope data (EA3). Major element compositions of all the ion microprobe analysis spot were obtained using electron microprobe prior to the isotope analyses and are shown in EA3. During analyses, utmost care was taken to locate clean surfaces on mineral phases in chondrules. However, SEM inspection of post-analysis ion microprobe spots led to the rejection of 30 out of 270 analyses because they overlapped with cracks, grain boundary, and inclusions. With the exception of ALL-2-CH-27 (IA), in which four out of six analyzed spots were rejected, at least five data were obtained from each chondrule after the spot evaluation.

3.1. Oxygen isotope ratios in porphyritic chondrules

3.1.1. Isotopically homogeneous chondrules

The oxygen three-isotope ratios of olivine grains in 27 type I and II porphyritic chondrules have a wide range of $\delta^{18}\text{O}$ and $\delta^{17}\text{O}$ values from $\sim -28.7\text{‰}$ to $\sim +5.3\text{‰}$ and from $\sim -30.2\text{‰}$ to $\sim +1.9\text{‰}$, respectively, which corresponds to $\Delta^{17}\text{O}$ from $\sim -17.7\text{‰}$ to $\sim +0.3\text{‰}$. The largest ^{16}O enrichments ($\delta^{18}\text{O}$ and $\delta^{17}\text{O} \sim -30\text{‰}$) were observed from olivine grains in two type IA chondrules, 3510-CH-8 and ALL-2-CH-33 (Fig. 2a), which are likely relict olivine grains similar to those found in Mokoia chondrules (Jones et al., 2004). In contrast, the highest $\Delta^{17}\text{O}$ value of $+0.3\text{‰}$ is observed from a large dusty olivine grain in ALL-2-CH-25 (IA), which is also considered to be a relict (EA1 and Fig. 1a). The spread of data among olivine in other porphyritic chondrules is limited mainly between $\delta^{18}\text{O} \sim -8\text{‰}$ to $\sim +3\text{‰}$, $\delta^{17}\text{O} \sim -10\text{‰}$ to $\sim -1\text{‰}$, and $\Delta^{17}\text{O} \sim -7\text{‰}$ to -2‰ (Fig. 2b), which overlaps with the range observed for the majority of chondrules in carbonaceous chondrites (e.g., Krot et al., 2006, references therein). The same limited range was also observed in low-Ca pyroxene, high-Ca pyroxene, and spinel in these chondrules (Fig. 2b). These data plot between the CCAM and Y&R lines, as observed in chondrules from Acfer 094 (Ushikubo et al., 2011). Only one plagioclase datum was obtained from 3658-CH-17 (IAB), which is on the CCAM line, but is off the trend from other minerals.

Among 26 porphyritic type I chondrules (excluding ALL-2-CH-27 with only 2 data), 17 chondrules (8 IA, 6 IAB, 1 IB, 1 IIA, and 1 IIAB) show homogeneous $\Delta^{17}\text{O}$ values for olivine, low-Ca pyroxene, high-Ca pyroxene, and spinel within each chondrule, as indicated from 2SD values of less than 1‰ (EA3). For these chondrules, the average oxygen isotope ratios are calculated and the results are shown in Table 2 and Fig. 3. In 3658-CH-17, $\Delta^{17}\text{O}$ values of high-Ca pyroxene and plagioclase are different from those in olivine and low-Ca pyroxene, so that the average oxygen

isotope ratios were calculated from olivine and low-Ca pyroxene data. In addition to these 17 chondrules, the $\Delta^{17}\text{O}$ values of 4 out of 5 olivine data in ALL-1-CH-4 (IA) are indistinguishable at $-5.1 \pm 0.3\text{‰}$ (2SD); the outlier being a relict olivine grain with a $\Delta^{17}\text{O}$ value of -6.7‰ (EA3). The average oxygen isotope ratio in this chondrule was calculated using the four similar measurements. The uncertainties of the average oxygen isotope ratios were estimated from twice the standard error of the mean (2SE) of multiple data (n), unless it is smaller than the weighted average of data. Additional 0.3‰ and 0.15‰ uncertainties in instrumental bias corrections for $\delta^{18}\text{O}$ and $\delta^{17}\text{O}$, respectively, are propagated to the final average values (EA3), as described in detail by Kita et al. (2010). The average $\Delta^{17}\text{O}$ values cluster at $-5.2 \pm 0.6\text{‰}$ (2SD) for 13 type I chondrules, while 5 other chondrules including both types I and II show $\Delta^{17}\text{O}$ values between -3‰ and -2‰ , which is similar to the distribution of the oxygen isotope ratios of chondrules from Acfer 094 (Ushikubo et al., 2011).

For these homogeneous porphyritic chondrules, the $\Delta^{17}\text{O}$ values in pyroxene, spinel and plagioclase are compared to those in olivine in the same chondrules (Fig. 4). In general, the oxygen isotope ratios of low-Ca and high-Ca pyroxene are indistinguishable and fall within the range of olivine data. The same is true for spinel. An exception is the case for high-Ca pyroxene and plagioclase analyzed in 3658-CH-17 (IAB), which show elevated $\Delta^{17}\text{O}$ values of $-3.8 \pm 0.5\text{‰}$ and $-2.5 \pm 0.5\text{‰}$ compared to those in olivine and low-Ca pyroxene with $\Delta^{17}\text{O}$ value of $-4.6 \pm 0.3\text{‰}$ (2SD, n=6).

3.1.2. Isotopically heterogeneous chondrules

Nine chondrules show internal heterogeneity in $\Delta^{17}\text{O}$ of more than 1‰, which are clearly resolved beyond the precision of the analyses (Fig. 5). Two type IA chondrules (3510-CH-8 and ALL-2-CH-33) contain extremely ^{16}O -rich olivine grains with $\Delta^{17}\text{O}$ value as low as -18‰ , though their chemical compositions are similar to other olivine grains present in the same chondrules (EA3). In ALL-1-CH-4 (IA) there is one relatively ^{16}O -rich olivine ($\Delta^{17}\text{O} = -6.7\text{‰}$) compared to other olivines with homogeneous oxygen isotope ratios of $\Delta^{17}\text{O} = -5.1 \pm 0.3\text{‰}$ (2SD, n=4). In 3510-CH-10 (IA), $\Delta^{17}\text{O}$ values of two larger olivine phenocrysts ($\Delta^{17}\text{O}$ of -2.7‰ and -2.5‰) are higher than three other olivine grains with the average $\Delta^{17}\text{O} = -6.1 \pm 0.4\text{‰}$ (2SD, n=3). In ALL-2-CH-30 (IA), one low-Ca pyroxene has the lowest $\Delta^{17}\text{O}$ (-4.1‰) and 7 olivine data range from -3.1‰ to -0.3‰ with four data clustered at -2.0‰ . The dusty olivine grain texture in ALL-2-CH-25 (IA) is zoned in FeO from Fa_7 in cores to Fa_4 at rims (Fig. 6a), which is FeO-enriched compared to olivine grains in the same chondrule ($<\text{Fa}_2$); these textural composition are similar to dusty olivine grains in other

studies (e.g. Jones and Danielson, 1997; Ruzicka et al., 2007). The dusty olivine grain ($\sim 150 \mu\text{m}$, Fig. 6a) is not supposed to have undergone melting during the last chondrule forming stage. The size of the relict grain is large compared to the average size of the other olivine grains ($\sim 50 \mu\text{m}$) in the chondrule. The $\Delta^{17}\text{O}$ values of core (Fa_7) and rim (Fa_4) of the dusty olivine are $+0.3\text{‰}$ and -1.3‰ , respectively, while those of the other Mg-rich host olivine grains ($\text{Fa}_{0.4}\text{--}\text{Fa}_2$) are from -4.9‰ to -3.7‰ (Fig. 6a).

In three type IIA chondrules, oxygen isotope ratios in relict grains generally correlate with zoning in Fo compositions. ALL-1-CH-32 (IIA) contains strongly zoned forsteritic core ($\text{Fo}_{80}\text{--}\text{Fo}_{90}$) in more FeO-rich olivine ($\text{Fo}_{60}\text{--}\text{Fo}_{64}$). The average $\Delta^{17}\text{O}$ value of two analyses from the forsteritic core region is -5.6‰ , which is significantly more ^{16}O -rich than the host olivine with the $\Delta^{17}\text{O}$ value of -2.5‰ (Fig. 6b). Olivine phenocrysts in ALL-1-CH-13 are typically zoned from $\text{Fo}_{64}\text{--}\text{Fo}_{73}$ and range in $\Delta^{17}\text{O}$ from -4.0‰ to -3.7‰ at the core of Mg-rich phenocrysts ($>\text{Fo}_{70}$), while host olivine and low-Ca pyroxene show homogeneous $\Delta^{17}\text{O}$ values of $-3.2 \pm 0.3\text{‰}$ (2SD, $n=4$) except for one olivine phenocryst (Fo_{66}) with a $\Delta^{17}\text{O}$ value of -2.3‰ (EA1 and EA3). 3510-CH-43 (IIA) contains a large phenocryst ($200 \mu\text{m} \times 100 \mu\text{m}$; Fig. 1f) which is more Mg-rich (Fo_{78}) when compared to other olivine grains in the same chondrule ($\text{Fo}_{60}\text{--}\text{Fo}_{63}$). In contrast to the case of other type IIA chondrules, this large olivine grain is relatively ^{16}O -poor, with a $\Delta^{17}\text{O}$ value of $-2.1 \pm 0.3\text{‰}$ (2SD, $n=3$), while the other olivine grains have a $\Delta^{17}\text{O}$ value of $-3.7 \pm 0.3\text{‰}$ (2SD, $n=3$) (EA3).

3.2. Oxygen isotope ratios in plagioclase rich chondrules

Plagioclase rich chondrules (PRC) are very rarely found in the Allende chondrite. The lone PRC ALL-2-CH-5 analyzed has large plagioclase grains ($>30 \mu\text{m}$) along with low-Ca and high-Ca pyroxene (EA1). This chondrule does not contain olivine. The plagioclase is anorthitic with a composition $\text{An}_{84}\text{--}\text{An}_{92}$. The pyroxene is typically FeO-poor, with compositions ranging from $\text{Fs}_1\text{--}\text{Fs}_3$. We could analyze only one low-Ca pyroxene, as it was difficult to find a clean surface. The oxygen isotope compositions of low-Ca pyroxene plot in the range similar to type I chondrules with $\Delta^{17}\text{O} \sim -5\text{‰}$ (Fig. 7). The oxygen isotope compositions of plagioclase in the PRC are very homogeneous with average values of $\delta^{18}\text{O} \sim +5.0 \pm 0.3\text{‰}$, $\delta^{17}\text{O} \sim 0.0 \pm 0.2\text{‰}$, and $\Delta^{17}\text{O} \sim -2.7 \pm 0.2\text{‰}$ (2SE), but differ significantly from pyroxene values (Fig. 7). The plagioclase data in the PRC are indistinguishable from that in porphyritic chondrule 3658-CH-17 (EA1 and EA3). In both cases, plagioclase data are significantly different from olivine and low-Ca pyroxene phenocrysts in the same chondrule.

3.3. Oxygen isotope ratios in barred olivine chondrules

Four FeO-poor (type I) barred olivine chondrule (ALL-1-CH-15, ALL-2-CH-9, 3510-CH-5, 3510-CH-41) were analyzed for oxygen three isotopes, as olivine bars were large enough ($>20\ \mu\text{m}$) for ion microprobe analysis (EA1). The texture of BO chondrules exhibits some variability (see EA1). Chondrule ALL-1-CH-15 has parallel bars of olivine that are not zoned (Fig. 1g). Chondrule ALL-2-CH-9 has a pyroxene rim and some of the olivine bars are not parallel and intercept each other in few places. Chondrule 3510-CH-5 has a rim that consists of olivine grains. Chondrule 3510-CH-41 contains a spinel grain. Multiple oxygen isotope analyses in each chondrule were indistinguishable within analytical uncertainties, indicating that olivine, low-Ca pyroxene, and spinel are homogeneous within the respective BO chondrules. The average oxygen isotope ratios of all the BO chondrules are shown in Fig. 7, which span over 10‰ in $\delta^{18}\text{O}$ and $\delta^{17}\text{O}$. Two of the four, ALL-2-CH-9 and 3510-CH-5, have average $\Delta^{17}\text{O}$ close to -5‰ i.e. $-5.2 \pm 0.3\text{‰}$ and $-5.6 \pm 0.3\text{‰}$, respectively (Fig. 8). The average $\Delta^{17}\text{O}$ value of 3510-CH-41 is intermediate at $-3.6 \pm 0.2\text{‰}$ and that of ALL-1-CH-15 is $-0.06\text{‰} \pm 0.11\text{‰}$, which plot on the TF line (Fig. 8).

The oxygen isotope ratios in a spinel grain and olivine in chondrule 3510-CH-41 are indistinguishable (Fig. 4 and EA3), suggesting that the spinel crystallized in the BO chondrule melt.

3.4. Oxygen isotope ratios in type I chondrule fragments

Oxygen isotope compositions of four type I chondrule fragments (IF) found in the matrix of the Allende chondrite were analyzed, and are illustrated in Fig. 7. Chemical compositions of Mg-rich olivine grains in IFs are homogenous, and range in composition from Mg# 90 to 99. The 5–6 analyses of oxygen isotopes were done on each of these IFs. Within each IF, the oxygen isotope ratios were homogeneous. The average $\delta^{18}\text{O}$, $\delta^{17}\text{O}$, and $\Delta^{17}\text{O}$ values range from -8.6‰ to -3.2‰ , -9.6‰ to -6.5‰ , and -6.0‰ to -4.3‰ , respectively (Fig. 7 and 8). The average $\Delta^{17}\text{O}$ from four IFs is $-5.3 \pm 0.8\text{‰}$ (2SD), which is indistinguishable from that of the -5‰ group in type I porphyritic chondrules.

In 3658-CH-5, pyroxene at the rim surrounding the olivine grain (EA1) was also analyzed, and is indistinguishable in $\Delta^{17}\text{O}$ from that of olivine, though significantly light oxygen isotope enriched (Fig. 7 and EA3). The $\delta^{18}\text{O}$ in pyroxene is $\sim 3\text{‰}$ lower than that of olivine (-8.6‰ versus -5.8‰), indicating that there could be the effect of mass dependent fractionation if pyroxene formed from the same oxygen isotope reservoir.

4. DISCUSSION

4.1. Oxygen isotope reservoirs for Allende Chondrules

In our study of the Allende chondrite 26 chondrules (including 4 BO and 4 IF) from total of 36 chondrules analyzed show internally homogeneous $\Delta^{17}\text{O}$ values with a 2SD smaller than 1‰. The average $\Delta^{17}\text{O}$ values in these chondrules are shown in Fig. 8. The histograms of $\Delta^{17}\text{O}$ values of homogeneous chondrules, as well as olivine data from internally heterogeneous type I and II porphyritic chondrules are shown in Fig. 9. Among them, 19 type I chondrules (including 2 BO and all IF) cluster at -5‰ with an average of $-5.3 \pm 0.6\text{‰}$ (2SD; Fig. 8). Most other chondrules range between -3.6‰ and -2‰ and one BO chondrule (ALL-1-CH-15) plots at 0‰ . The distribution of $\Delta^{17}\text{O}$ values in Allende chondrules in Fig. 8 and Fig. 9a are similar to those in Acfer 094 by Ushikubo et al. (2011), showing a bimodal distribution at $-5.3 \pm 1.2\text{‰}$ (2SD, $n=19$) and $-2.2 \pm 0.7\text{‰}$ (2SD, $n=16$). In Acfer 094, the former group consists of chondrules exclusively with $\text{Mg}\#>96$, while the latter group includes both type I and II chondrules with a wide range of $\text{Mg}\#$. In isotopically homogeneous Allende chondrules, the $\text{Mg}\#$ in olivine may have been modified by parent body metamorphism, but chondrules with $\Delta^{17}\text{O}$ values of -5‰ are always type I chondrules. Compared to the Acfer 094 data, the Allende chondrules that fall in -5.3‰ group show a narrower distribution of oxygen isotopes ($\pm 0.6\text{‰}$ for Allende, while $\pm 1.2\text{‰}$ for Acfer 094), while the -2‰ group is not so obvious (Figs. 8 and 9a). In four heterogeneous chondrules (3510-CH-10, ALL-1-CH-32, 3510-CH-43, and ALL-1-CH-13), the highest $\Delta^{17}\text{O}$ values among olivine data are at -2‰ , while the lowest value ranges between -6‰ and -4‰ (Fig. 5). Thus, these chondrules show a similar bimodal distribution at -5‰ and -2‰ within a chondrule, which is often related to distinct chemical or petrographical characteristics of olivine grains. Relict olivine grains in type I chondrules show a broad peak at around -2‰ (Fig. 9b), which indicates that chondrules in Allende contain precursor solids with $\Delta^{17}\text{O}$ values of -2‰ .

Ushikubo et al. (2011) suggested that Acfer 094 chondrules formed in two oxygen isotope reservoirs under dust-rich environments (e.g., Cuzzi and Alexander, 2006), in which oxygen isotope ratios of ambient gas during chondrule forming heating events are similar to those of the average dust. Two different oxygen isotope reservoirs may represent isotope heterogeneity in the localized disk regions, from which the Acfer 094 parent asteroid formed. Our new data from Allende chondrules strongly indicate a common oxygen isotope reservoir with $\Delta^{17}\text{O} = -5\text{‰}$ for chondrule forming regions of both the Acfer 094 and Allende chondrites. A minor group of chondrules in Allende formed in a relatively ^{16}O -depleted isotope reservoir with a $\Delta^{17}\text{O}$ of -2‰ . Chondrules with

internally heterogeneous oxygen isotope ratios often show a range of $\Delta^{17}\text{O}$ values between -5‰ and -2‰ , which might have resulted from mixing of these two isotope reservoirs (Figs. 5 and 9).

There is also a hint of third oxygen isotope reservoir at $\sim 0\text{‰}$ that falls on the terrestrial fractionation (TF) line, according to data from one BO chondrule (ALL-1-CH-15; Fig. 7) and relict olivine grains in three IA chondrules (ALL-2-CH-25, ALL-2-CH-30, ALL-2-CH-33; Fig. 5), one of which contains a dusty olivine grain. Acfer 094 also contains a minor amount of chondrules with the same isotopic signature. These data are very similar to those of bulk FeO-rich BO chondrules (Clayton et al., 1983) which have an average $\Delta^{17}\text{O}$ value of $-0.60 \pm 0.23\text{‰}$ ($n=6$).

As clearly shown in Fig. 9, $\Delta^{17}\text{O}$ values of homogeneous chondrules in this work (Fig. 9a) are very different from those of bulk CV3 chondrules from the literature (Fig. 9d; Clayton et al., 1983; Rubin et al., 1990; Jones et al., 2004). The bulk chondrule data are systematically higher in $\Delta^{17}\text{O}$ values and do not show any peak at -5‰ . One possible explanation for this discrepancy is that the bulk data are biased towards higher $\Delta^{17}\text{O}$ values due to the contribution from altered mesostasis. In earlier ion microprobe analyses of olivine and magnetite in Allende chondrules, Choi et al. (1997) found that the olivine data in 4 PO chondrules are systematically lower in $\Delta^{17}\text{O}$ values (-5.7 to -4.1‰) than bulk measurements, which was suggested to be caused by contribution of altered mesostasis with a higher $\Delta^{17}\text{O}$ value, indicated from magnetite data in the meteorite ($\sim -2\text{‰}$). Indeed, plagioclase data from two chondrules (ALL-2-CH-5 and 3658-CH-17) show similar $\Delta^{17}\text{O}$ values ($-2.7 \pm 0.2\text{‰}$ and $-2.5 \pm 0.5\text{‰}$, respectively) that are different from those of olivine and pyroxene in the same chondrules. The unequilibrated ordinary chondrites (UOCs) also have ^{16}O -poor mesostasis (plagioclase/glass) compared to olivine and pyroxene due to isotopic exchange (Sears et al., 1998; Bridges et al., 1999; Kita et al. 2010).

4.2. Origin of relict olivine in porphyritic chondrules

Two chondrules 3510-CH-8 and ALL-2-CH-33 show a significantly large internal variation in oxygen isotope ratios and contain significantly ^{16}O -rich olivine grains ($\Delta^{17}\text{O}$ values ranging from -18‰ to -11‰), which are likely relict material (Fig 5). A similar range of ^{16}O -rich olivine in chondrules are not commonly observed; only a limited number of cases were found in the Yamato-81020 CO3 chondrite (Chondrule I; Yurimoto and Wasson, 2002), Mokoia (Chondrule 11 and 12; Jones et al., 2004), and Acfer 094 (G68 and G70; Ushikubo et al., 2009; 2011). As discussed earlier (e.g., Yurimoto and Wasson, 2002; Jones et al., 2004), these ^{16}O -rich relict olivines might be related to refractory inclusions, such as amoeboid olivine aggregates (AOAs). The olivine grains with the extreme oxygen isotope ratios have major elemental compositions not different from those of other

grains in the same chondrules. Hence, it is difficult for us to relate individual relict grains to specific early generation objects according to the major element composition in olivine. This may be explained by homogenization of Fe-Mg diffusion of olivine at high temperature during chondrule formation, while retention of the distinct oxygen isotope ratios due to the slow diffusion rate of oxygen (Jones et al., 2004).

It is interesting to note that one olivine grain in ALL-2-CH-33, which has the lowest $\Delta^{17}\text{O}$ value among all the analyses in this study ($-17.7 \pm 0.4\%$), plots on the oxygen three-isotope diagram significantly displaced from the CCAM line by $\sim +10\%$ in $\delta^{18}\text{O}$ if it is mass dependent isotope fractionation (Fig. 2a). This displacement from the CCAM line may be due to Rayleigh type evaporation processes during the formation of the precursor of the relict grain predating the formation of the ALL-2-CH-33 chondrule. For this relict olivine grain, the CaO content (0.75%) is much higher than those in other olivine grains ($\leq 0.3\%$). A High CaO content of the olivine may indicate that the relict olivine grain formed in Ca, Al-rich melt at high temperature, in which Rayleigh type distillation would have occurred.

Excluding the rare examples of relict olivine grains with oxygen isotope ratios close to those of refractory inclusions, relict olivine grains in Allende chondrules studied here show a range of $\Delta^{17}\text{O}$ values very similar to those in homogeneous chondrules (Figs. 5 and 9). Similar results were reported by Ushikubo et al. (2011) from Acfer 094 chondrules. These results support the idea that relict grains in chondrules were derived from previously formed chondrules (Nagahara, 1981; Jones, 1996; Jones and Danielson, 1997).

Chaussidon et al. (2008) suggested that olivine grains in type IA chondrules in CV and CR chondrites are relict grains that formed originally in igneously differentiated planetary bodies. They claimed that during chondrule formation, olivine grains reacted with SiO gas in the solar nebula to form pyroxene. According to their ion microprobe oxygen isotope analyses of olivine and pyroxene in CR and CV chondrules, they observed a relationship between oxygen isotope ratios in olivine (Ol) and pyroxene (Px) as follows: $\delta^{18}\text{O}(\text{Px}) = 0.72 \times \delta^{18}\text{O}(\text{Ol}) + 1.21$ and $\delta^{17}\text{O}(\text{Px}) = 0.81 \times \delta^{17}\text{O}(\text{Ol}) + 0.60$. In Fig. 10, we plot $\delta^{18}\text{O}$ and $\delta^{17}\text{O}$ values of olivine and pyroxene in the same chondrules to test this relationship. Our data plot on 1:1 line, i.e. $\delta^{18}\text{O}(\text{Px}) = \delta^{18}\text{O}(\text{Ol})$ and $\delta^{17}\text{O}(\text{Px}) = \delta^{17}\text{O}(\text{Ol})$, which contradicts the equations in Chaussidon et al. (2008). There are two exceptions that plot below and above 1:1 lines in Fig. 10. These data are from 3658-CH-5 and ALL-1-CH-20, in which the $\delta^{18}\text{O}$ and $\delta^{17}\text{O}$ data in low-Ca pyroxene are mass fractionated relative to olivine with indistinguishable $\Delta^{17}\text{O}$ values, which could be caused by kinetic or equilibrium fractionation between chondrule melt

and ambient gas (Kita et al., 2010). Thus, these data do not follow the equations given by Chaussidon et al. (2008) that are not caused by mass dependent isotope fractionation.

Recently, Libourel and Chaussidon (2011) reported $\Delta^{17}\text{O}$ values of olivine grains from type I chondrules and fragments in Allende having peaks at -6‰ to -5‰ . Although these olivine grains are hypothesized to be relict olivine with planetary origins, their $\Delta^{17}\text{O}$ values completely overlap with those of most type I chondrules with homogeneous isotope ratios shown in Fig. 8. Thus, we do not find any evidence to support a planetary origin for relict olivine grains.

4.3. The Oxygen isotope composition in Barred Olivine chondrules

Our FeO-poor BO chondrule data show a large range of $\Delta^{17}\text{O}$ values from -5.6‰ to 0‰ (Fig. 8). Two of the four data fall in the region similar to that of type I chondrules. These $\Delta^{17}\text{O}$ values are systematically lower than literature data on bulk BO chondrules in Allende ($\Delta^{17}\text{O}$ from -1.5‰ to -0.4‰ ; Clayton et al., 1983). It should be noted that BO chondrules analyzed by Clayton et al. (1983) were mainly FeO-rich BO chondrules, which we did not find from the sections we studied. There are a few bulk BO data with $\Delta^{17}\text{O}$ values of $\sim -4\text{‰}$ reported both by Clayton et al. (1983) and Jones et al. (2004). Ushikubo et al. (2011) also reported one FeO-poor BO chondrule in Acfer 094 with a $\Delta^{17}\text{O}$ value of -5.0‰ . Thus, BO chondrules may have a wider range of $\Delta^{17}\text{O}$ values than previously reported. Bulk BO chondrule data might be biased by alteration of mesostasis in Allende chondrules as discussed earlier. If parent body fluid had a $\Delta^{17}\text{O}$ value of $\sim -2\text{‰}$, as inferred from magnetite (Choi et al., 1997), oxygen isotope exchange between BO chondrules and fluid would result in shifting bulk $\Delta^{17}\text{O}$ values of BO chondrules towards -2‰ ; this would lower the bulk $\Delta^{17}\text{O}$ value for BO chondrules with $\Delta^{17}\text{O} \sim 0$, and would raise the bulk $\Delta^{17}\text{O}$ values for BO chondrules with $\Delta^{17}\text{O} < -3\text{‰}$.

The texture of BO chondrules indicates total melting of the chondrule precursor followed by fast cooling. Clayton et al. (1983) suggested that FeO-rich BO chondrules recorded the oxygen isotope ratios of the solar nebula gas that exchanged with chondrules during complete melting. From the narrow range of oxygen isotope ratios among bulk Allende BO chondrules, Clayton et al. (1983) concluded solar nebular gas has oxygen isotope ratios close to the TF line. If oxygen isotope ratios in BO chondrules represent those of solar nebula gas during chondrule formation, our new BO chondrule data with a wide range of $\Delta^{17}\text{O}$ values may indicate multiple oxygen isotope reservoirs for chondrule formation. It is possible that bulk BO data from Clayton et al. (1983) are biased towards one of many isotope reservoirs due to preferential selection of FeO-rich BO chondrules that could be large enough for bulk analyses.

4.4. The Oxygen isotope composition of spinel in Allende chondrules

Spinel is not typically found in ferromagnesian chondrules, and its presence may indicate that it could be a relict grain from CAIs or that it may have crystallized from chondrule melt (Sheng et al., 1991; Ma et al., 2008). Maruyama et al. (1999) reported two cases from Allende chondrules, where a PRC contains ^{16}O -rich spinel that might be a relict from CAIs, and a spinel-bearing BO chondrule where the spinel oxygen isotope ratios are indistinguishable from those in olivine. In our Allende study, three type I chondrules (ALL-1-CH-9, 3510-CH-3, and 3510-CH-41) contain spinel grains (Fig. 11) that have indistinguishable oxygen isotope ratios from those in olivine (Fig. 7 and EA3). The BSE images of 3510-CH-41 show olivine enclosed by spinel (Figs. 11e and f). Thus, occurrence of spinel grains in 3510-CH-41 suggests that the spinel grains were formed during the last chondrule melting event. In addition, Cr_2O_3 concentrations in our spinel grains are higher ($> 0.5\text{wt}\%$) than those of CAI spinels ($< 0.5\text{wt}\%$) and within the range of spinel co-crystallized with olivine in chondrules (Ma et al., 2008). It is concluded that the spinel grains in the three chondrules were “home-grown” (Maruyama et al., 1999; Maruyama and Yurimoto, 2003; Ma et al. 2008) and not incorporated from early generation objects like CAIs.

4.5. The Oxygen isotope composition of plagioclase in Allende chondrules

Plagioclase analyses from two chondrules, ALL-2-CH-5 (PRC) and 3658-CH-17 (IAB), have similar oxygen isotope ratios (EA3), with weighted average $\delta^{18}\text{O}$, $\delta^{17}\text{O}$, and $\Delta^{17}\text{O}$ values of $5.1 \pm 0.2\text{‰}$, $0.0 \pm 0.4\text{‰}$, and $-2.6 \pm 0.4\text{‰}$, respectively. When compared to olivine and pyroxene within the same chondrules, plagioclase data are significantly depleted in ^{16}O and they plot on the other side of the CCAM line (Figs. 2b, 4 and 7). Since plagioclase is one of the last minerals to crystallize in chondrules it is likely to have near-complete oxygen isotopic exchange and homogenization with nebular gas. However, the chondrules in Allende have experienced metamorphism in the presence of fluid, resulting in alteration to various degrees (Krot et al., 1995, 1997). Phyllosilicates and other hydrous minerals are rarely observed in Allende (Tomeoka and Buseck, 1982; Kimura and Ikeda, 1998; Brearley, 1997), though later thermal metamorphism in the parent body might have dehydrated the phases (Krot et al., 1998a, 1998b). The temperature of metamorphism for the Allende meteorite has been estimated to be between 340 °C (Brearley, 1997) and 600 °C (Huss and Lewis, 1994). At this temperature range, oxygen isotopes in $10\text{ }\mu\text{m}$ sized anorthitic plagioclase could be homogenized on the time scale of 0.1–10 million years by applying the experimentally determined self-diffusion rates of Ryerson and McKeegan (1994). In contrast, self-diffusion rates of oxygen in olivine and

pyroxene are several orders magnitude lower than anorthite (e.g., Cole and Chakraborty, 2001), so that oxygen isotope ratios recorded in these minerals during chondrule formation would not be affected by parent body metamorphism.

Analyses of chondrule mesostasis by ion microprobe (Maruyama et al., 1999) or altered mesostasis rich areas using in-situ laser fluorination analyses in Allende (Ash et al., 1999; Ash and Young, 2000) indicate that the $\Delta^{17}\text{O}$ value of fluid is $\sim -3\%$. Choi et al. (1997) reported oxygen isotope analyses of magnetite in Allende with $\Delta^{17}\text{O}$ values $\sim -2\%$ (actual data range from -0.4 to -2.6%), which represent those of water that oxidized metal in the Allende parent body. The $\Delta^{17}\text{O}$ values of our plagioclase data are very similar to those in altered mesostasis and magnetite in the meteorite, strongly indicating that plagioclase in Allende chondrules exchanged oxygen isotope nearly completely with the aqueous fluid.

4.6. Oxygen isotope trend in Allende CV chondrules

A compilation of 225 oxygen isotope analyses of olivine and pyroxene from a wide variety of chondrules (type I and II and its sub-type) from the Allende chondrite is plotted as a function of $\delta^{18}\text{O}$ versus $\delta^{17}\text{O}$ in Fig. 12. Olivine data from ALL-2-CH-33 (spot #4) were not included in the regression line because the data show extremely ^{16}O -rich isotope signature and also mass dependent fractionation. The plagioclase data have been excluded as it may have been affected by aqueous alteration in the parent body. Spinel is not typically found in chondrules; hence it is also not considered. Excluding plagioclase and spinel, the slope of the chondrule data is 0.98 ± 0.02 (regression line: $\delta^{17}\text{O} = (0.982 \pm 0.019) \times \delta^{18}\text{O} - (2.91 \pm 0.10)$ and MSWD = 4.4 using ISOPLOT; Ludwig, 2003). The regression line is similar to the compiled bulk data of Mokoia and Allende chondrules ($\delta^{17}\text{O} = 0.99 \times \delta^{18}\text{O} - 3.48$) measured by Jones et al. (2004). This result is almost the same as the PCM (primitive chondrule mineral) line from Acfer 094 chondrules (regression line: $\delta^{17}\text{O} = (0.987 \pm 0.013) \times \delta^{18}\text{O} - (2.70 \pm 0.11)$, Ushikubo et al., 2011). The Y intercept of the regression line locates above the CCAM line by $\sim 1\%$ and below the Y&R line by $\sim 2\%$. The results in this study further confirm the previous observation by Ushikubo et al. (2011) that the trend of oxygen isotope ratios of chondrules from carbonaceous chondrites are significantly displaced from the CCAM and Y&R line.

5. CONCLUSIONS

In-situ analyses of oxygen three-isotope ratios were performed on 36 chondrules from the Allende CV3.2 chondrite, sampling a wide variety of chondrules on different minerals using the ion microprobe. The following conclusions were drawn.

1. The oxygen isotope ratios in olivine, pyroxene, and spinel within the same chondrule are indistinguishable except for relict olivine grains. These results indicate that minerals formed from a melt with homogeneous oxygen isotope ratios, which reflect the ambient gas during the high temperature chondrule-forming events.
2. The Allende chondrules show two main groups of oxygen isotope ratios, clustering at $\Delta^{17}\text{O} \sim -5\text{‰}$ and -2‰ . The observed bimodal distribution is similar to that of Acfer 094 chondrules (Ushikubo et al., 2011). The bimodal distribution of the oxygen isotope ratios observed in the Allende chondrules may represent those in the local dust-rich protoplanetary disk, from which the CV3 parent asteroid formed.
3. Rare extremely ^{16}O -rich relict olivine grains in Allende chondrules may be related to refractory precursors similar to CAIs and AOAs. However, the majority of relict olivine grains exhibit a similar range of $\Delta^{17}\text{O}$ values when compared to homogeneous chondrules, indicating that they derived from previously formed chondrules in the same regions.
4. The observed oxygen isotope ratios of BO chondrules have a wide range of $\Delta^{17}\text{O}$ values from -5‰ to 0‰ , indicating that not all BO chondrules are ^{16}O -poor and near the TF line as suggested by previous bulk analyses (e.g. Clayton et al., 1983; Jones et al., 2004). The variation of oxygen isotopes among BO chondrules implies the existence of multiple oxygen isotope reservoirs for the formation of CV3 chondrules.
5. The compilation of 225 olivine and pyroxene measurements lie on the line $\delta^{17}\text{O} = (0.982 \pm 0.019) \times \delta^{18}\text{O} - (2.91 \pm 0.10)$. This slope is similar to the compiled bulk data of Mokoia and Allende chondrules by Jones et al. (2004) and in situ analysis of Acfer 094 chondrule by Ushikubo et al. (2011). These data deviate significantly from the Y&R line and plot slightly above CCAM line.

ACKNOWLEDGEMENTS

We thank Glenn MacPherson and Linda Welzenbach, Smithsonian Institute, for the use of two Allende thin sections. We thank J. N. Goswami, Physical Research Laboratory, Ahmedabad for providing Allende samples for this study. We thank Brian Hess for preparation of two polished sections and Jim Kern for technical support. The assistance of John Fournelle for the SEM and electron microprobe analysis is gratefully acknowledged. Travis Tenner is acknowledged for his comments on the draft of the manuscript. We are grateful to Sara Russell, Hajime Hiyagon and Hisayoshi Yurimoto for their useful reviews. NGR thanks the Director, NIO, Goa for the support. This work is supported by the NASA Cosmochemistry Program (NNX07AI46G, NNX10AH77G; NK). WiscSIMS is partly supported by NSF (EAR03-19230, EAR07-44079).

Electronic Annex

EA1: BSE images of individual chondrules and ion microprobe analysis spots.

EA2: Electron microprobe analyses of mineral phases in chondrules.

EA3: Oxygen three isotope analyses of chondrules.

REFERENCES

- Ash R. D. and Young E. D. (2000) Clarity and confusion: the history of Allende chondrules as evinced by oxygen isotopes. *Lunar Planet. Sci.* **31** (Abstract #1881).
- Ash R. D., Young E. D., Rumble III, D., Alexander C. M. O'D. and MacPherson G. J. (1999) Oxygen isotope systematics in Allende chondrules. *Lunar Planet. Sci.* **30** (Abstract #1836).
- Brearley A. J. (1997) Disordered biopyriboles, amphibole, and talc in the Allende meteorite: Products of nebular or parent body aqueous alteration? *Science* **276**, 1103–1105.
- Bridges J.C., Franchi I.A., Sexton A.S. and Pillinger C.T. (1999) Mineralogical controls on the oxygen isotopic compositions of UOCs, *Geochim. Cosmochim. Acta* **63**, 945–951.
- Chaussidon M., Libourel G. and Krot A. N. (2008) Oxygen isotopic constraints on the origin of magnesian chondrules and on the gaseous reservoirs in the early Solar System. *Geochim. Cosmochim. Acta* **72**, 1924–1938.

- Choi B. G., McKeegan K. D., Leshin L. A. and Wasson J. T. (1997) Origin of magnetite in oxidized CV chondrites: in situ measurement of oxygen isotope compositions of Allende magnetite and olivine. *Earth Planet. Sci. Lett.* **146**, 337–349.
- Clayton R. N. (1993) Oxygen isotopes in meteorites. *Annu. Rev. Earth Planet. Sci.* **21**, 115–149.
- Clayton R. N., Grossman L. and Mayeda T. K. (1973) A component of primitive nuclear composition in carbonaceous meteorites. *Science* **182**, 485–488.
- Clayton R. N., Onuma N., Grossman L. and Mayeda T. K. (1977). Distribution of pre-solar component in Allende and other carbonaceous chondrites. *Earth Planet. Sci. Lett.* **34**, 209–224.
- Clayton R. N., Onuma N., Ikeda Y., Mayeda T. K., Hutcheon I. D., Olsen E. J. and Molini-Velsko C. (1983) Oxygen isotopic compositions of chondrules in Allende and ordinary chondrites. In *Chondrules and Their Origins* (ed. E. A. King), pp. 37–43. Lunar and Planetary Institute, Houston.
- Cole D. R. and Chakraborty S. (2001) Rates and mechanisms of isotopic exchange. In *Stable Isotope Geochemistry* (eds. by J. W. Valley and S. R. Cole), Reviews in Mineralogy and Geochemistry 43, pp.83-223.
- Cuzzi J. N. and Alexander C. M. O'D. (2006) Chondrule formation in particle-rich nebular regions at least hundreds of kilometres across. *Nature* **441**, 483-485.
- Heck P. R., Ushikubo T., Schmitz B., Kita N. T., Spicuzza J. M. and Valley J. W. (2010) A single asteroidal source for extraterrestrial Ordovician chromite grains from Sweden and China: High-precision oxygen three isotope SIMS analysis. *Geochim. Cosmochim. Acta* **74**, 497–509.
- Jabeen I., Kusakabe M., Nakamura T. and Nagao K. (1998a) Oxygen isotopic signature in Allende chondrules. *Meteorit. Planet. Sci.* **33** (Suppl.), A76–A77.
- Jabeen I., Kusakabe M., Nakamura T. and Nagao K. (1998b) Oxygen isotope study of Tsukuba chondrite, some HED meteorites and Allende chondrules. *Antarct. Meteorite Res.* **11**, 122–135.
- Jones R. H. (1996) Relict grains in chondrules: Evidence for chondrule recycling. In *Chondrules and the Protoplanetary Disk* (eds. R. H. Hewins et al.), pp. 163–172. Cambridge University Press.
- Jones R. H. and Danielson L. R. (1997) A chondrule origin for dusty RELICT olivine in unequilibrated chondrites. *Meteor. Planet. Sci.* **32**, 753–760.
- Jones R. H., Leshin L. A., Guan Y., Sharp Z. D., Durakiewicz T. and Schilk A. J. (2004) Oxygen isotope heterogeneity in chondrules from the Mokoia CV3 carbonaceous chondrite. *Geochim. Cosmochim. Acta* **68**, 3423–3438.

- Kimura M. and Ikeda Y. (1998) Hydrous and anhydrous alterations of chondrules in Kaba and Mokoia CV chondrites. *Meteor. Planet. Sci.* **33**, 1139–1146.
- Kita N. T., Nagahara H., Togashi S. and Morishita Y. (2000) A short duration of chondrule formation in the solar nebula: evidence from ^{26}Al in Semarkona ferromagnesian chondrules. *Geochim. Cosmochim. Acta* **64**(22), 3913–3922.
- Kita N. T., Ushikubo T., Fu B. and Valley J. W. (2009) High precision SIMS oxygen isotope analysis and the effect of sample topography. *Chemical Geology* **264**, 43–57.
- Kita N. T., Nagahara H., Tachibana S., Tomomura S., Spicuzza M. J., Fournelle J. H. and Valley J. W. (2010) High precision SIMS oxygen three isotope study of chondrules in LL3 chondrites: Role of ambient gas during chondrule formation. *Geochim. Cosmochim. Acta* **74**, 6610–6635.
- Krot A. N., Scott E. R. D. and Zolensky M. E. (1995) Mineralogical and chemical modification of components in CV3 chondrites: Nebular or asteroidal processing? *Meteoritics* **30**, 748–775.
- Krot A. N., Scott E. R. D. and Zolensky M. E. (1997) Origin of fayalitic olivine rims and lath-shaped matrix olivine in the CV3 chondrite Allende and its dark inclusions. *Meteoritics* **32**, 31–49.
- Krot A. N., Petaev M. I., Scott E. R. D., Choi B. G., Zolensky M. E. and Keil K. (1998a) Progressive alteration in CV3 chondrites: More evidence for asteroidal alteration. *Meteorit. Planet. Sci.* **33**, 1065–1085.
- Krot A. N., Petaev M. I., Zolensky M. E., Keil K., Scott E. R. D. and Nakamura K. (1998b) Secondary Ca-Fe-rich minerals in the Bali-like and Allende-like oxidized CV3 chondrites and Allende dark inclusions. *Meteorit. Planet. Sci.* **33**, 625–645.
- Krot A. N., Yurimoto H., McKeegan K. D., Leshin L., Chaussidon M., Libourel G., Yoshitake M., Huss G. R., Guan Y. B. and Zanda B. (2006) Oxygen isotopic compositions of chondrules: Implications for evolution of oxygen isotopic reservoirs in the inner solar nebula. *Chem. Erde* **66**, 249–276.
- Krot A. N., Nagashima K., Yoshitake M. and Yurimoto H. (2010) Oxygen isotopic compositions of chondrules from the metal-rich chondrites Isheyevo (CH/CB_b), MAC 02675 (CB_b) and QUE 94627 (CB_b). *Geochim. Cosmochim. Acta* **74**, 2190–2211.
- Kurahashi E., Kita N. T., Nagahara H. and Morishita Y. (2008) ^{26}Al – ^{26}Mg systematics of chondrules in a primitive CO chondrite. *Geochim. Cosmochim. Acta* **72**, 3865–3882.
- Libourel G. and Chaussidon M. (2011) Oxygen isotopic constraints on the origin of Mg-rich olivines from chondritic meteorites. *Earth Planet. Sci. Lett.* **301**, 9–21.
- Libourel G. and Krot A. N. (2007) Evidence for the presence of planetesimal material among the precursors of magnesian chondrules of nebular origin. *Earth Planet. Sci. Lett.* **254**, 1–8.

- Lyons J. R. and Young E. D. (2005) CO self-shielding as the origin of oxygen isotope anomalies in the early solar nebula. *Nature* **435**, 317–320.
- Ludwig K. R. (2003) Isoplot 3.00 A geochronological toolkit for Microsoft excel. Berkeley Geochronology Center Special Publication No.4, 1–72.
- Ma C., Beckett J. R., Connolly H. C. Jr. and Rossman G. R. (2008) Aluminous spinels in ferromagnesian chondrules from Allende. *Lunar Planet. Sci.* **39**, #2030 (abstr.).
- Maruyama S. and Yurimoto H. (2003) Relationship among O, Mg isotopes and the petrography of two spinel-bearing compound chondrules. *Geochim. Cosmochim. Acta* **67**, 3943-3957.
- Maruyama S., Yurimoto H. and Sueno S. (1999) Oxygen isotope evidence regarding the formation of spinel-bearing chondrules. *Earth Planet. Sci. Lett.* **169**, 165–171.
- Nagahara H. (1981) Evidence for secondary origin of chondrules. *Nature* **292**, 135-136.
- Nakamura T., Noguchi T., Tsuchiyama A., Ushikubo T., Kita N. T., Valley J. W., Zolensky M. E., Kakazu Y., Sakamoto K., Mashio E., Uesugi K. and Nakano T. (2008) Chondrulelike objects in short-period comet 81P/Wild 2. *Science* **321**, 1664–1667.
- Ryerson, F. J. and McKeegan K. D. (1994) Determination of oxygen self-diffusion in åkermanite, anorthite, diopside, and spinel: Implications for oxygen isotopic anomalies and the thermal histories of Ca-Al-rich inclusions. *Geochim. Cosmochim. Acta* **58**, 3713-3734.
- Rubin A. E., Wasson J. T., Clayton R. N. and Mayeda T. K. (1990) Oxygen isotopes in chondrules and coarse-grained chondrule rims from the Allende meteorite. *Earth Planet. Sci. Lett.* **96**, 247–255.
- Rudraswami N. G. and Goswami J. N. (2007) ²⁶Al in chondrules from unequilibrated L chondrites: onset and duration of chondrule formation in the early solar system. *Earth Planet. Sci. Lett.* **257**, 231–244.
- Rudraswami N. G., Goswami J. N., Chattopadhyay B., Sengupta S. K. and Thapliyal A. P. (2008) ²⁶Al records in chondrules from unequilibrated ordinary chondrites: II. Duration of chondrule formation and parent body thermal metamorphism. *Earth Planet. Sci. Lett.* **274**, 93–102.
- Ruzicka A., Hiyagon H., Hutson M. and Floss C. (2007) Relict olivine, chondrule recycling, and the evolution of nebular oxygen reservoirs. *Earth Planet. Sci. Lett.* **257**, 274-289.
- Sears D. W. G., Lyon I., Saxton J. and Turner G. (1998) The oxygen isotopic properties of olivines in the Semarkona ordinary chondrite. *Meteorit. Planet. Sci.* **33**, 1029–1032.
- Sheng Y. J., Hutcheon I. D. and Wasserburg G. J. (1991) Origin of plagioclase-olivine inclusions in carbonaceous chondrites. *Geochim. Cosmochim. Acta* **55**, 581-599.

- Thiemens M. H. and Heidenreich J. E. (1983) The mass-independent fractionation of oxygen: a novel isotope effect and its possible cosmochemical implications. *Science* **219**, 1073–1076.
- Tomeoka K. and Buseck P. R. (1982) An unusual layered mineral in chondrules and aggregates of the Allende carbonaceous chondrite. *Nature* **299**, 327–329.
- Ushikubo T., Kimura M., Kita N. T., and Valley J. W. (2009) Oxygen isotopic compositions of phenocrysts in chondrules from the primitive carbonaceous chondrite Acfer 094. *Lunar Planet. Sci.* **40**, Abstr. #1383.
- Ushikubo T., Kimura M., Kita, N.T., and Valley, J.W. (2011). Primordial oxygen isotope reservoirs of the solar nebula recorded in chondrules in Acfer 094 carbonaceous chondrite. *Lunar Planet. Sci.* **42**, Abstr. #1183.
- Valley J. W. and Kita N. (2009) In situ oxygen isotope geochemistry by ion microprobe. Mineralogical Association of Canada Short Course 41, Toronto, May 2009, pp.19–63.
- Young E. D. and Russell S. S. (1998) Oxygen reservoirs in the early solar nebula inferred from an Allende CAI. *Science* **282**, 452–455.
- Young E. D., Galy A., and Nagahara H. (2002) Kinetic and equilibrium mass-dependent isotope fractionation laws in nature and their geochemical and cosmochemical consequences. *Geochim. Cosmochim. Acta* **66**, 1095–1104.
- Yu Y., Hewins R. H., Clayton R. N. and Mayeda T. K. (1995) Experimental study of high temperature oxygen isotope exchange during chondrule formation. *Geochim. Cosmochim. Acta* **59**, 2095–2104.
- Yurimoto H. and Kuramoto K. (2004) Molecular cloud origin for the oxygen isotope heterogeneity in the solar system. *Science* **305**, 1763–1766.
- Yurimoto H. and Wasson J. T. (2002) Extremely rapid cooling of a carbonaceous-chondrite chondrule containing very ^{16}O -rich olivine and a ^{26}Mg excess. *Geochim. Cosmochim. Acta* **66**, 4355–4363.

Figure Captions

Fig. 1. Representative backscattered electron (BSE) images of analyzed Allende chondrules using ion microprobe. The BSE images (minerals abbreviations: Ol=olivine, Lpx=low-Ca pyroxene, Hpx=high-Ca pyroxene, Pl=plagioclase) are shown with scale bars of 100 μm . (a) ALL-2-CH-25 (IA), (b) 3658-CH-8 (IA), (c) 3658-CH-17 (IAB), (d) ALL-2-CH-3 (IAB), (e) ALL-1-CH-32 (IIA), (f) 3510-CH-43 (IIA), (g) ALL-1-CH-15 (BO), and (h) ALL-2-CH-20 (IF).

Fig. 2. Oxygen three-isotope ratios of porphyritic chondrules. Data are shown in EA3. (a) Chondrules with extreme ^{16}O -rich relict olivine grains. Olivine data from 3510-CH-8 (IA) and ALL-2-CH-33 (IA) are shown as triangle and inverted-triangle symbols. Olivine data from other porphyritic type I chondrules are shown as small squares. TF ($\delta^{17}\text{O} = 0.52 \times \delta^{18}\text{O}$), Y&R ($\delta^{17}\text{O} = 1.00 \times \delta^{18}\text{O} - 1.04$; Young and Russell, 1998), and CCAM ($\delta^{17}\text{O} = 0.94 \times \delta^{18}\text{O} - 4.1$; Clayton et al., 1977) lines are shown for reference. The ^{16}O -rich data from 3510-CH-8 fall between CCAM and Y&R lines, while that of ALL-2-CH33 plot significantly right of the CCAM line. (b) Oxygen isotope ratios of minerals in other porphyritic chondrules: olivine (squares), low-Ca pyroxene (circles), high-Ca pyroxene (triangles), spinel (diamonds), and plagioclase (inverted triangles). Except for plagioclase, all data plot between Y&R and CCAM lines.

Fig. 3. Oxygen three-isotope ratios of 18 individual porphyritic chondrules with internally homogeneous $\Delta^{17}\text{O}$ values. The average oxygen isotope ratios of each chondrule were calculated from olivine and pyroxene data (EA3 and Table 2). Types I and II chondrules are shown as open and filled squares, respectively, while literature bulk CV3 chondrule data are shown as grey squares (Clayton et al., 1983; Rubin et al., 1990; Jones et al. 2004). Data cluster in two regions corresponding to $\Delta^{17}\text{O}$ values of $\sim -5\text{‰}$ and $\sim -2\text{‰}$.

Fig. 4. The $\Delta^{17}\text{O}$ values of pyroxene, spinel, and plagioclase against those in olivine in the same porphyritic chondrules. Most data plot on 1:1 line, indicating olivine, pyroxene, and spinel were crystallized from the same chondrule melt with homogeneous oxygen isotope ratios. Exceptions are plagioclase and high-Ca pyroxene data in 3658-CH-17 (IAB), where plagioclase and high-Ca pyroxene data are ^{16}O -depleted compared to olivine data. Abbreviations: Lpx= low-Ca pyroxene; Hpx= high-Ca pyroxene; Pl= plagioclase; Sp= spinel.

Fig. 5. Porphyritic chondrules with internally heterogeneous $\Delta^{17}\text{O}$ values. Variations in $\Delta^{17}\text{O}$ values in each chondrule are shown. Olivine and pyroxene data are shown as open circles and filled inverted triangles, respectively. Three chondrules (ALL-2-CH-25, 3510-CH-43, and ALL-1-CH-32) contain possible xenolith grains that show distinct textures or chemical compositions, such as dusty olivine, a large olivine phenocryst, and a forsteritic olivine core (shown in rectangular box).

Fig. 6. BSE images of ALL-2-CH-25 (a), and ALL-1-CH-32 (b) with enlarged areas depicting dusty olivine (dusty Ol) and a large forsteritic olivine core, respectively. The BSE images are also marked with circles indicating the region of ion microprobe analysis with $\Delta^{17}\text{O}$ values.

Fig. 7. Oxygen three-isotope ratios of BO chondrules (ALL-1-CH-15, 3510-CH-41, 3510-CH-5, and ALL-2-CH-9), IFs (ALL-2-CH-20, 3658-CH-5, 3658-CH-23, and 3510-CH-19), and a PRC (ALL-2-CH-5) from the Allende CV3 chondrite. The average values are shown for most chondrules because they are internally homogeneous in $\Delta^{17}\text{O}$ values (Table 2). Plagioclase data in PRC are significantly ^{16}O -poor and differ from that of low-Ca pyroxene. For the 3658-CH-5 (IF), the low-Ca pyroxene (filled triangle) and the average olivine (open triangle) are connected by a dashed line. Note that the low-Ca pyroxene data in 3658-CH-5 are lighter than that of olivine and the two minerals are mass fractionated from each other. Except for ALL-1-CH-15 (BO), which is depleted in ^{16}O and falls on the TF line, all data plot within or close to the range observed for the majority of type I chondrules with $\Delta^{17}\text{O}$ value of -5‰ (shown as dashed ellipse). The bulk CV3 chondrules from literature are shown in grey squares (Clayton et al., 1983; Rubin et al., 1990; Jones et al., 2004).

Fig. 8. The $\Delta^{17}\text{O}$ values of 27 chondrules in Allende CV3. The average values are shown for 26 chondrules with homogeneous oxygen isotope ratios (18 porphyritic chondrules, 4 BO, and 4 IF). For ALL-2-CH-5 PRC the single measurement of low-Ca pyroxene (-4.6‰ ; EA3) was chosen to represent its average value because the plagioclase analyses might have been affected by parent body alteration (see text). The majority of chondrules plot between $\Delta^{17}\text{O}$ values of -6‰ and -4.5‰ (shaded area), similar to those found in majority of type I chondrules in Acfer 094 (Ushikubo et al., 2011). Others show higher $\Delta^{17}\text{O}$ values up to 0‰ . The dashed line represents $\Delta^{17}\text{O} = -2.2\text{‰}$, which is seen among type I and type II chondrules in Acfer 094 (Ushikubo et al., 2011), as well as chondrules in CR and CB chondrites (Krot et al., 2006, 2010).

Fig. 9. Histograms of $\Delta^{17}\text{O}$ values from Allende chondrules: (a) homogeneous chondrules (the averaged values), (b) individual spot analyses of heterogeneous type I chondrules, and (c) individual spot analyses of heterogeneous type II chondrules. The literature data for bulk chondrules in CV3 (Clayton et al., 1983, Rubin et al., 1990; Jones et al., 2004) are shown in (d) for reference.

Fig. 10. Comparison between oxygen isotope ratios of olivine and low-Ca pyroxene in the same porphyritic chondrules: (a) $\delta^{18}\text{O}$ and (b) $\delta^{17}\text{O}$. Most data plot on 1:1 line. Our data do not agree with the relationship between olivine and pyroxene reported by Chaussidon et al. (2008), which is shown as dashed line (labelled as “C08”).

Fig. 11. BSE images of type I chondrules ALL-1-CH-9, 3510-CH-3, and 3510-CH-41 that contain spinel grains. The rectangular regions are enlarged on the right hand side. The numbered filled circles represent spinel grains that were analyzed by the ion microprobe. The oxygen isotope data and chemical composition is given in EA3. The minerals abbreviations are: Sp=spinel and Ol=olivine.

Fig. 12. Oxygen isotope plot of 225 analyses from olivine and pyroxene from 36 Allende chondrules. The data are provided in electronic annex (EA3). One olivine measurement with an open circle symbol is from ALL-2-CH-33 (spot #4) that was not included in the estimation of the regression line. Errors reported are 2SD. Data fall between the CCAM and Y&R line (shown as dashed lines). The TF line is shown for reference. The regression line is depicted as the solid and is fit by the following equation: $\delta^{17}\text{O} = (0.982 \pm 0.019) \times \delta^{18}\text{O} - (2.91 \pm 0.10)$.

Table 1. Mineral Chemistry of chondrules from Allende selected for oxygen isotope studies.

Type	Chondrule	Mg#	Olivine	Low-Ca Pyroxene			Spinel	Plagioclase
			Fo%	Wo%	En%	Fs%	Mg#	An%
IA	ALL-1-CH-4	92.5	92.5	1.7	97.1	1.2	-	-
	ALL-1-CH-9	98.2	98.6	2.5	95.0	2.5	85.3	-
	ALL-1-CH-10	95.7	95.0	1.1	96.1	2.8	-	-
	ALL-1-CH-21	97.6	97.6	-	-	-	-	-
	ALL-2-CH-25	97.0	97.0	-	-	-	-	-
	ALL-2-CH-27	91.8	91.8	-	-	-	-	-
	ALL-2-CH-30	97.1	96.8	3.9	94.3	1.8	-	-
	ALL-2-CH-33	95.5	95.5	-	-	-	-	-
	3658-CH-8	96.8	96.8	-	-	-	-	-
	3658-CH-29	98.6	98.6	-	-	-	-	-
	3510-CH-3	99.1	99.5	-	-	-	89.2	-
	3510-CH-4	91.7	91.7	-	-	-	-	-
	3510-CH-8	92.4	92.4	-	-	-	-	-
	3510-CH-10	90.1	90.1	-	-	-	-	-
3510-CH-27	96.7	96.7	-	-	-	-	-	
IAB	ALL-1-CH-20	97.5	97.6	1.2	97.5	1.2	-	-
	ALL-2-CH-3	93.3	89.9	0.9	95.0	4.1	-	-
	ALL-2-CH-26	96.3	96.4	3.0	94.7	2.4	-	-
	3658-CH-17	95.6	92.7	2.4	95.4	2.2	-	85.7
	3658-CH-24	96.7	95.9	1.0	98.2	0.8	-	-
	3510-CH-21	96.2	95.4	1.2	97.4	1.3	-	-
IB	ALL-1-CH-24	92.5	-	0.9	96.4	2.7	-	-
PRC	ALL-2-CH-5	97.5	-	2.6	94.9	2.5	-	86.1
BO	ALL-1-CH-15	93.9	93.9	-	-	-	-	-
	ALL-2-CH-9	95.6	93.6	1.5	96.5	2.1	-	-
	3510-CH-5	98.1	98.1	-	-	-	-	-
	3510-CH-41	97.8	98.7	-	-	-	93.0	-
IF	ALL-2-CH-20	95.4	95.4	-	-	-	-	-
	3658-CH-5	96.3	95.5	1.4	96.9	1.7	-	-
	3658-CH-23	98.8	98.8	1.1	97.8	1.1	-	-
	3510-CH-19	97.9	97.7	1.1	97.6	1.2	-	-
IIA	ALL-1-CH-13	64.8	53-73	2.8	65.7	31.5	-	-
	ALL-1-CH-31	61.2	61.1	3.9	62.5	33.6	-	-
	ALL-1-CH-32	65.6	57-90	-	-	-	-	-
	3510-CH-43	66.8	56-78	-	-	-	-	-
IIAB	ALL-2-CH-16	68.2	58-73	1.5	71.9	26.5	-	-

Porphyritic chondrules are divided in Type I (FeO-poor; Mg# \geq 90) and Type II (FeO-rich; Mg# $<$ 90). Further division are: A (>80% olivine), AB (20-80% olivine) and B (<20% olivine). Other chondrule types in Allende include PRC (Plagioclase rich chondrule), BO (Barred olivine), IF (type I chondrule

fragments). Mg# is Molar Mg/(Fe+Mg) %. Mineral names are as follows: Fo=Forsterite, Fa=Fayalite, Wo= Wollastonite, En= Enstatite, Fs=Ferrosilite, Ab=Albite, An=Anorthite. Spinel is closed to MgAl₂O₄ end member with addition of hercynite component (FeAl₂O₄), which is indicated as Mg# given above.

Table 2. The average oxygen isotope compositions of individual chondrules excluding heterogeneous relict olivine grains

Type	Chondrule	n	$\delta^{18}\text{O}$	2 σ	$\delta^{17}\text{O}$	2 σ	$\Delta^{17}\text{O}$	2 σ
IA	ALL-1-CH-4	4	-3.62	0.44	-6.96	0.30	-5.08	0.17
	ALL-1-CH-9	8	-4.40	0.33	-7.58	0.22	-5.30	0.22
	ALL-1-CH-10	5	-4.87	0.52	-8.17	0.27	-5.64	0.14
	ALL-1-CH-21	8	-4.54	0.41	-7.57	0.25	-5.21	0.20
	3658-CH-8	6	-4.92	0.53	-7.82	0.36	-5.26	0.22
	3658-CH-29	6	0.44	0.42	-1.93	0.32	-2.16	0.21
	3510-CH-3	9	-7.41	0.40	-9.62	0.28	-5.76	0.14
	3510-CH-4	7	-5.38	0.58	-8.20	0.31	-5.40	0.23
	3510-CH-27	8	-6.36	0.37	-8.41	0.28	-5.11	0.25
IAB	ALL-1-CH-20	7	-3.85	0.82	-7.34	0.49	-5.33	0.22
	ALL-2-CH-3	7	0.42	0.42	-2.33	0.24	-2.55	0.16
	ALL-2-CH-26	7	-4.57	0.32	-7.44	0.29	-5.06	0.19
	3658-CH-17	6	-3.54	0.51	-6.47	0.33	-4.63	0.21
	3658-CH-24	7	-5.23	0.35	-8.25	0.25	-5.53	0.20
	3510-CH-21	6	0.57	0.47	-2.58	0.49	-2.87	0.31
IB	ALL-1-CH-24	6	-3.69	0.39	-6.74	0.28	-4.82	0.23
BO	ALL-1-CH-15	6	3.81	0.39	1.92	0.25	-0.06	0.11
	ALL-2-CH-9	8	-4.73	0.42	-7.71	0.32	-5.25	0.26
	3510-CH-5	8	-5.86	0.40	-8.64	0.32	-5.59	0.26
	3510-CH-41	7	-2.83	0.42	-5.10	0.31	-3.63	0.17
IF	ALL-2-CH-20	6	-5.09	0.33	-8.29	0.23	-5.64	0.19
	3658-CH-5	5	-5.76	0.33	-8.55	0.23	-5.56	0.24
	3658-CH-23	5	-4.40	0.33	-7.35	0.24	-5.06	0.24
	3510-CH-19	5	-3.49	0.47	-6.68	0.35	-4.86	0.31
IIA	ALL-1-CH-31	6	1.74	0.33	-1.22	0.21	-2.12	0.12
IIAB	ALL-2-CH-16	8	0.48	0.55	-2.98	0.37	-3.24	0.18

Calculation and error estimates of the average values of individual chondrules are shown in EA3.

Fig. 1

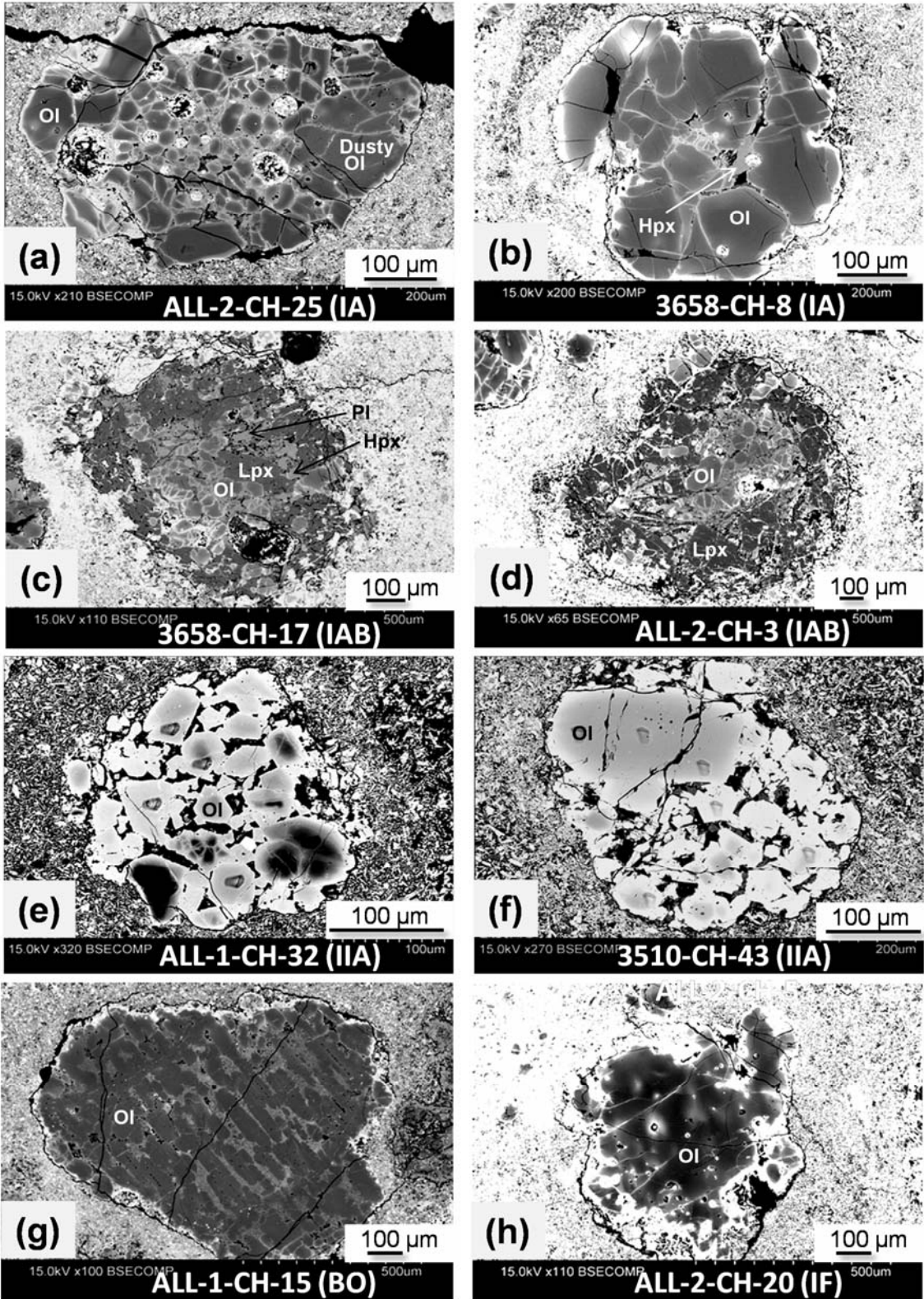


Fig. 2a

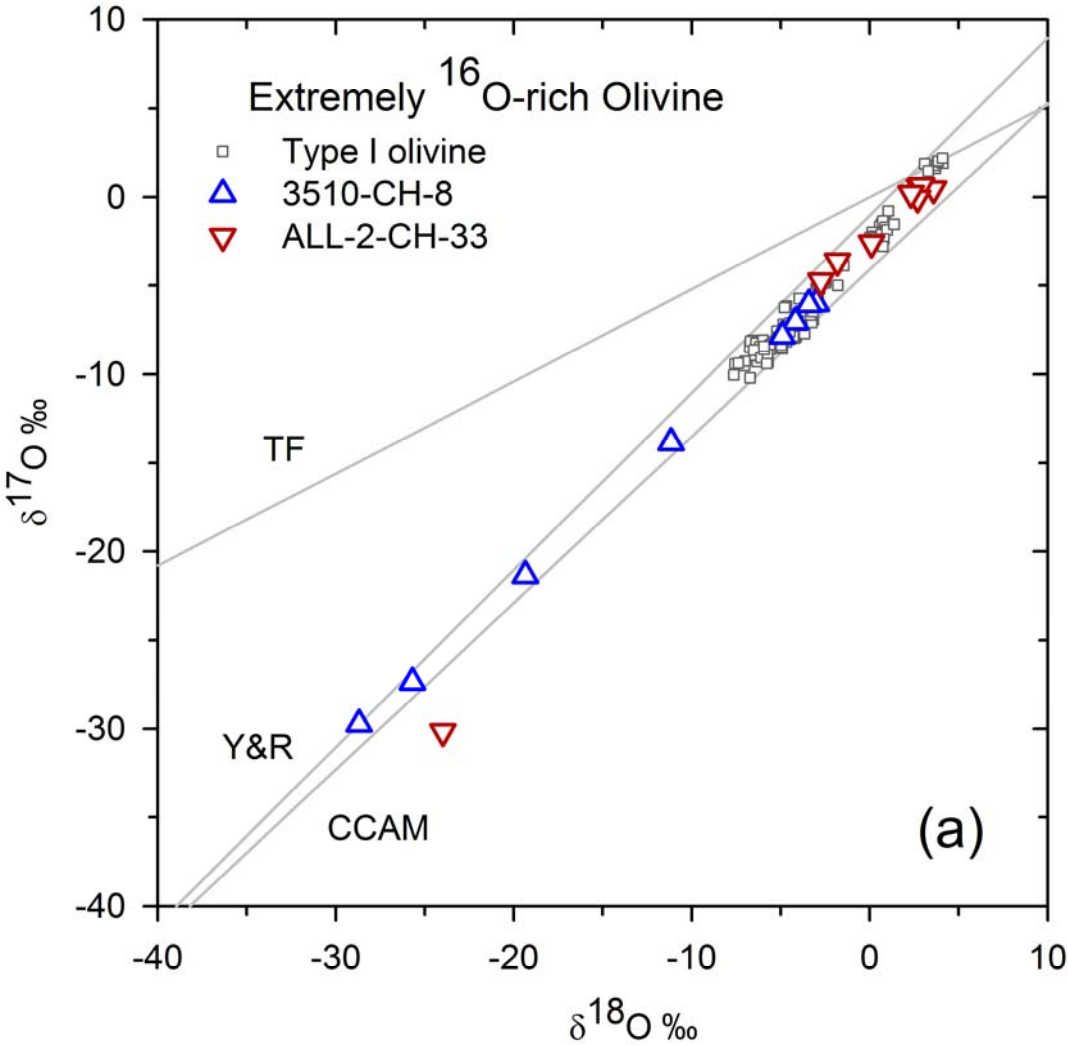


Fig. 2b

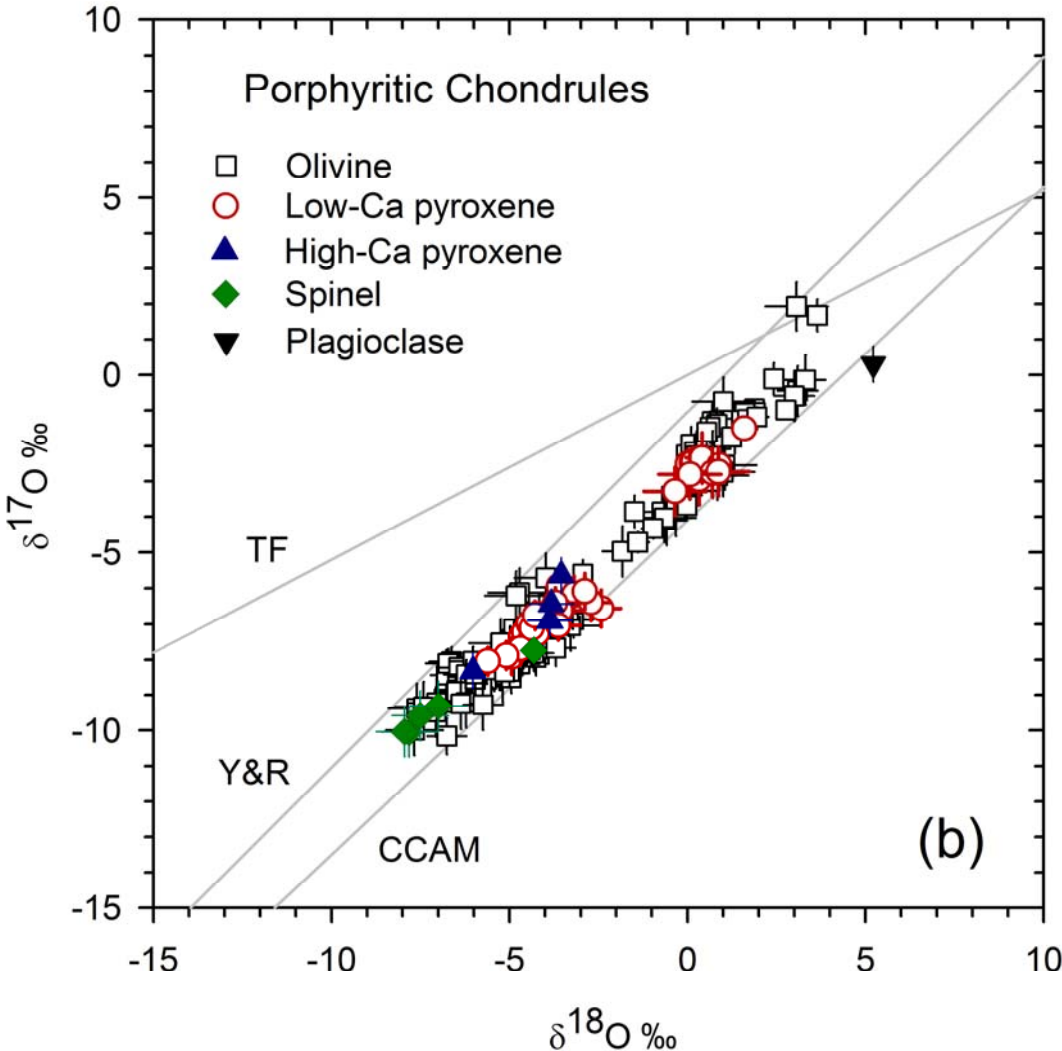


Fig. 3

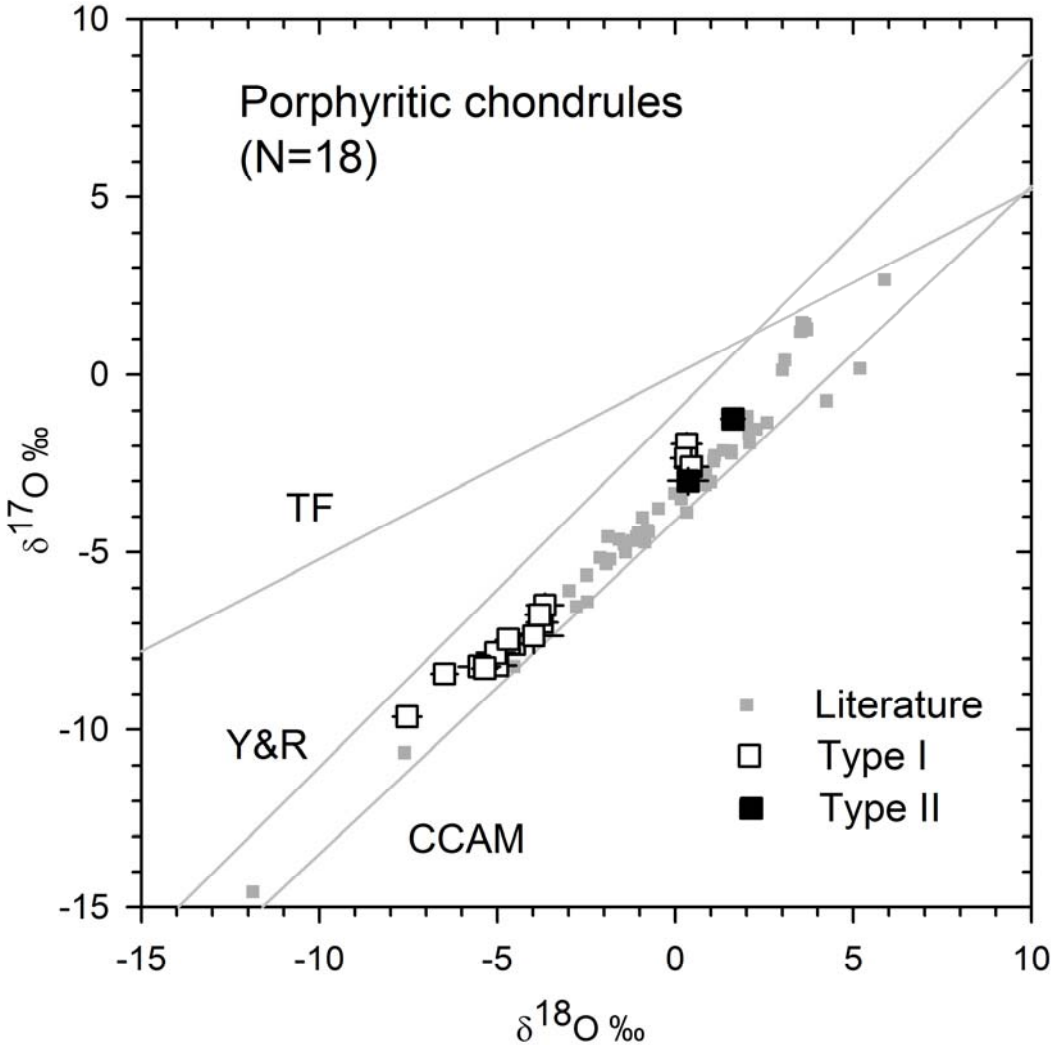


Fig. 4

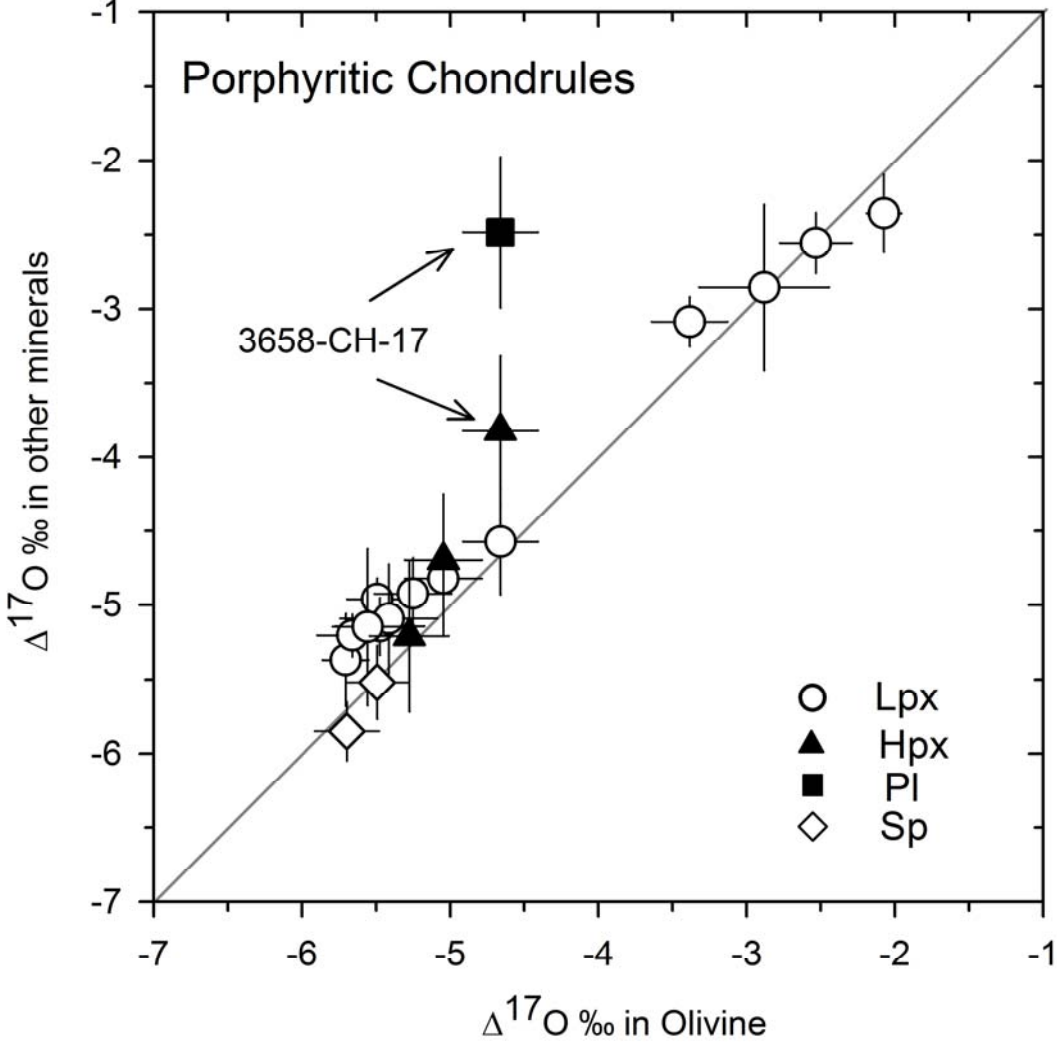


Fig. 5

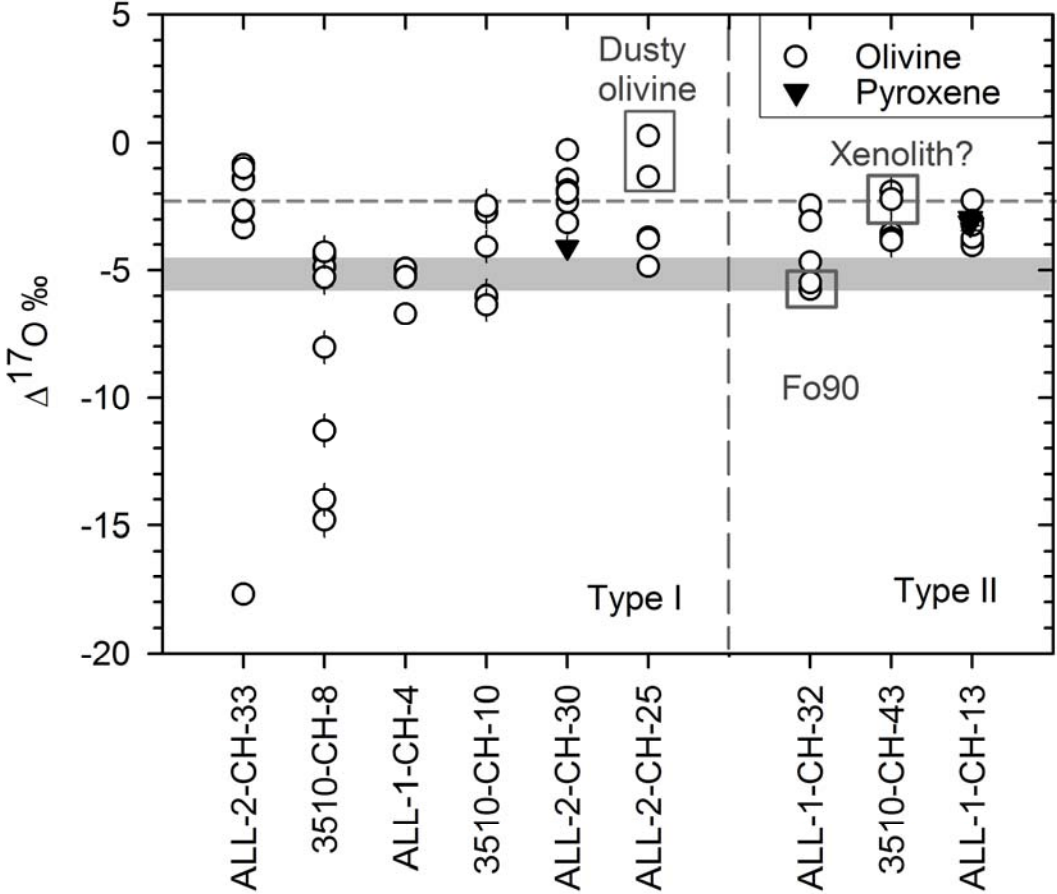


Fig. 6

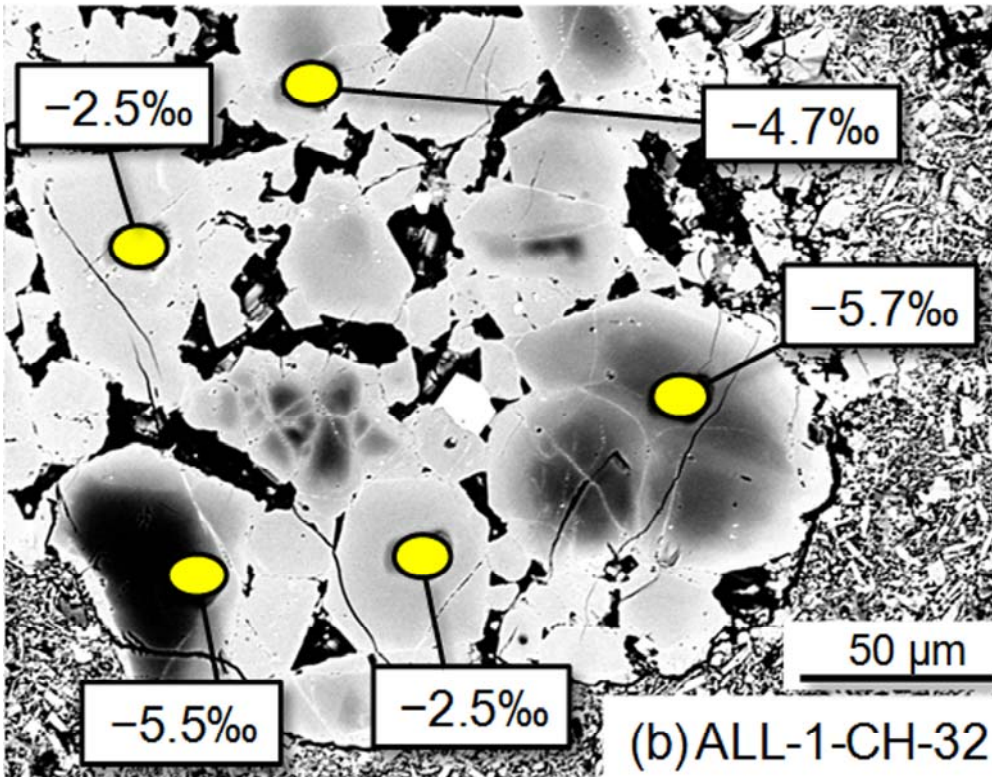
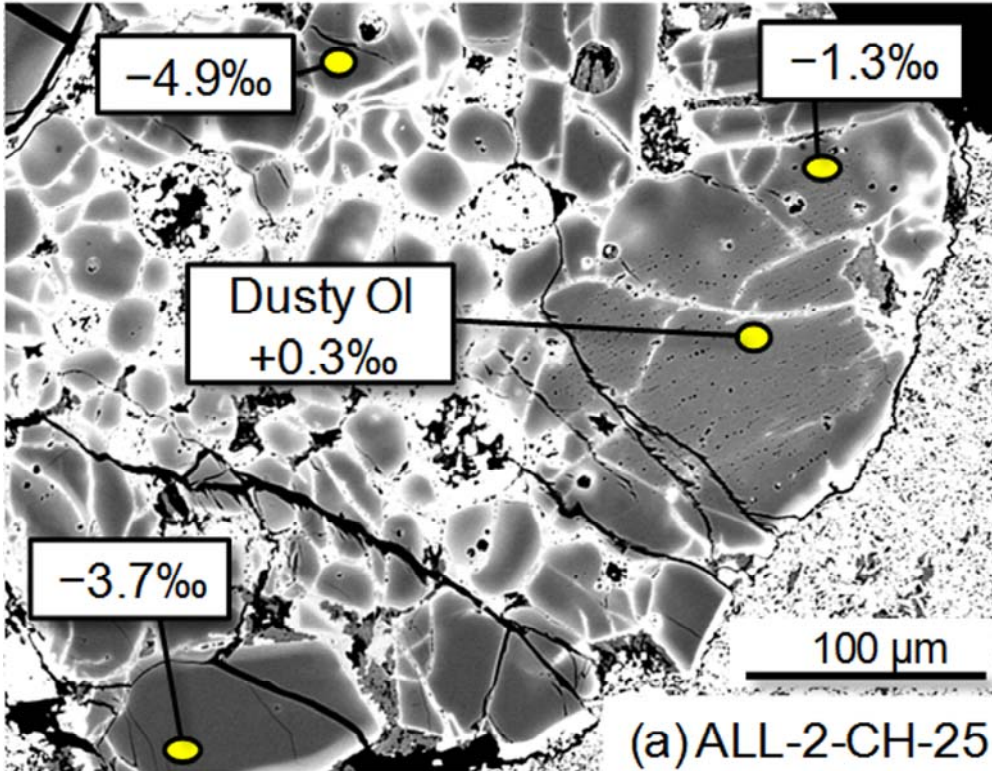


Fig. 7

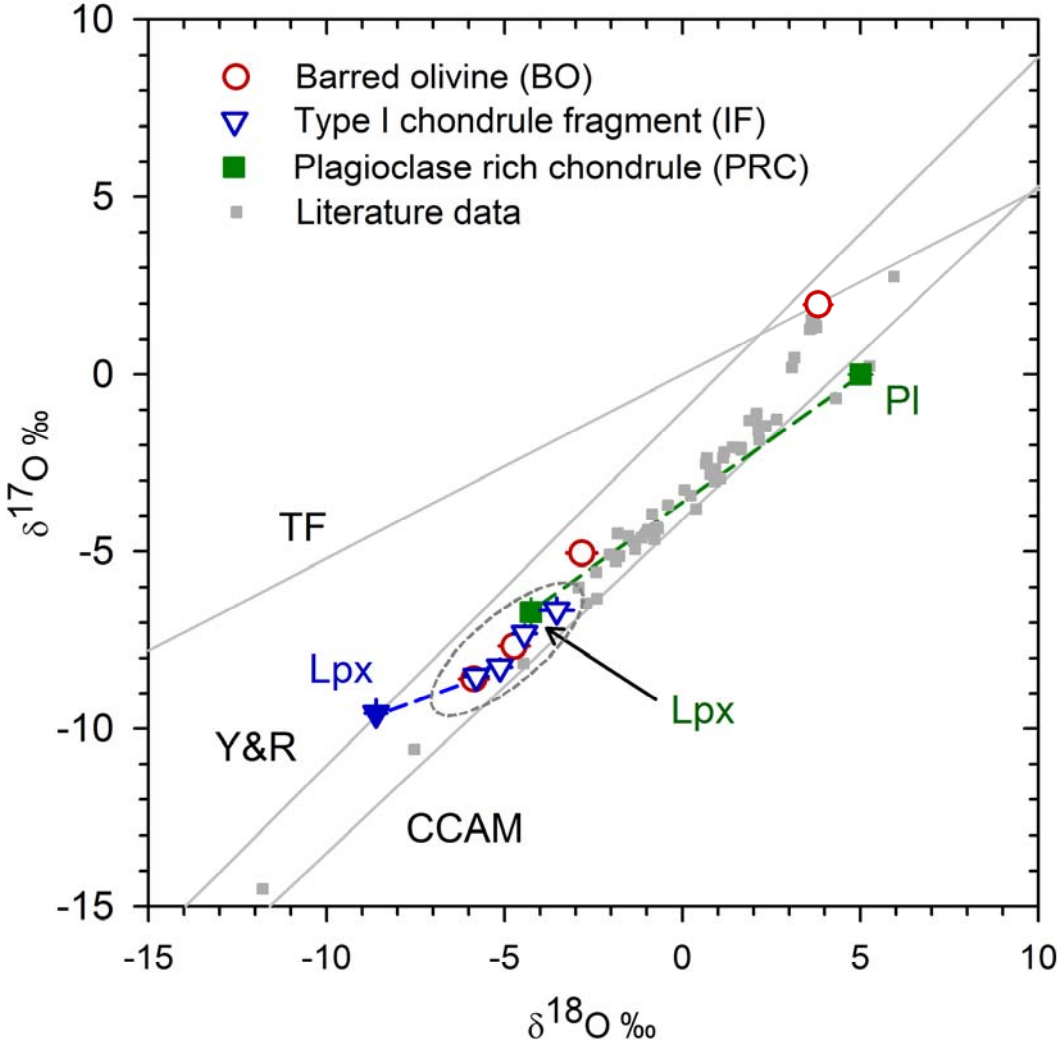


Fig. 8

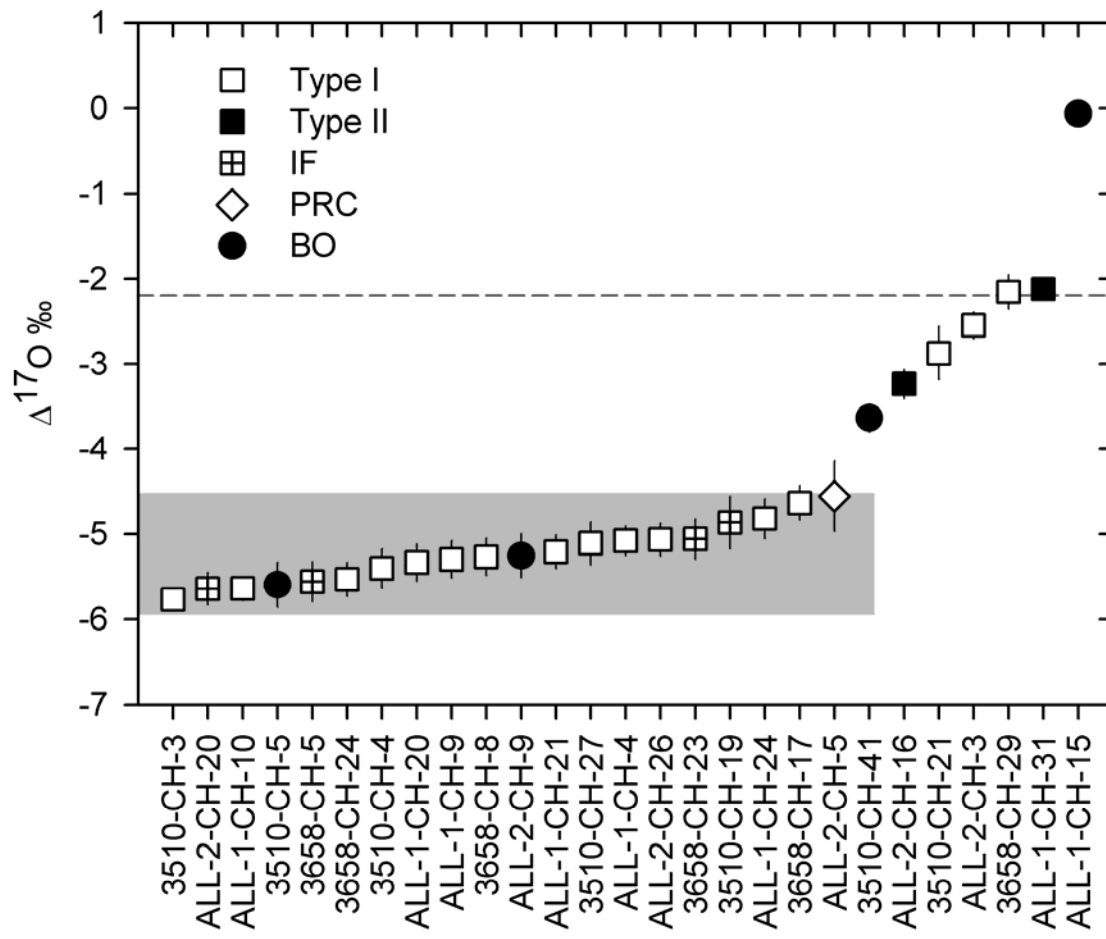


Fig. 9

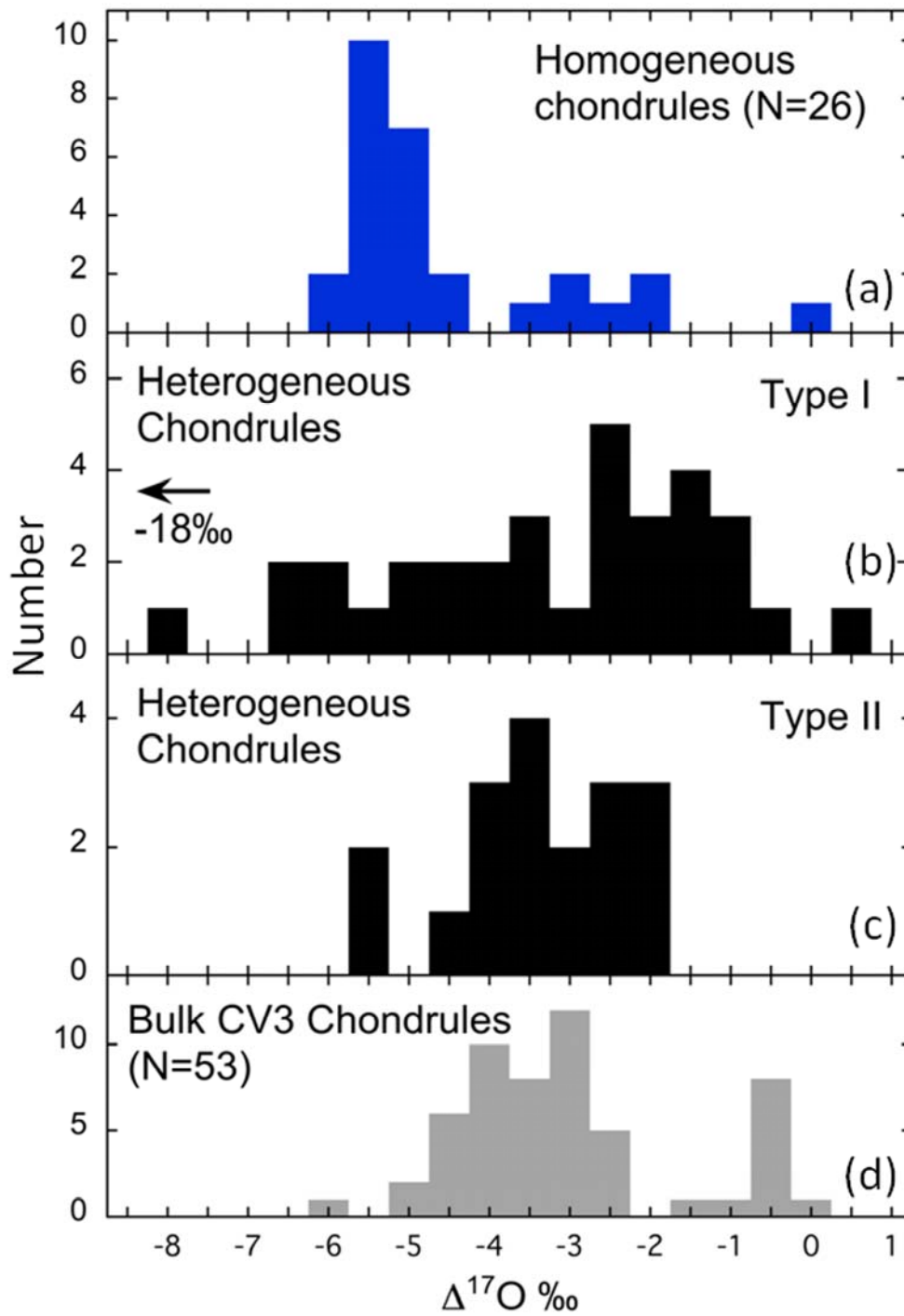


Fig. 10

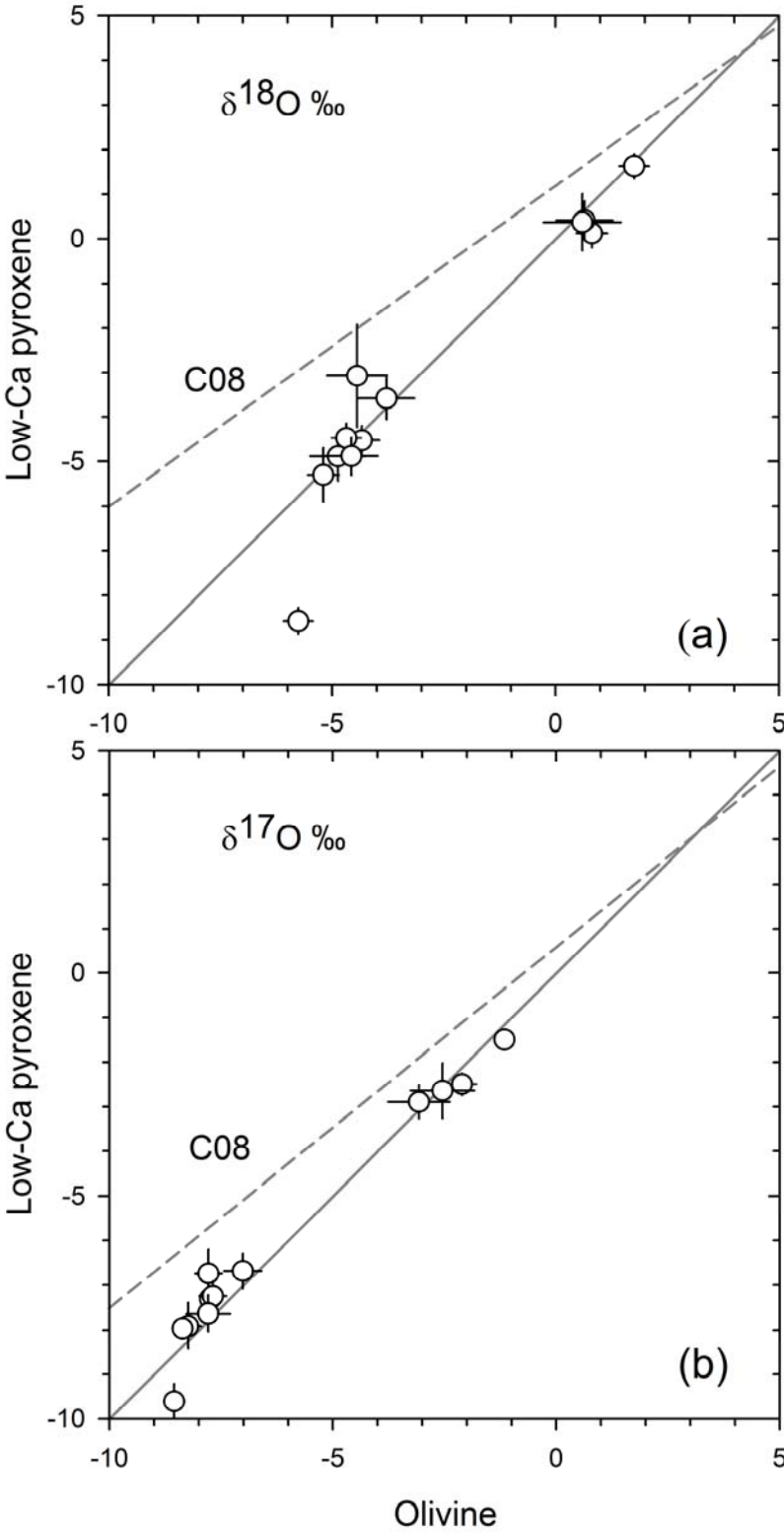


Fig. 11

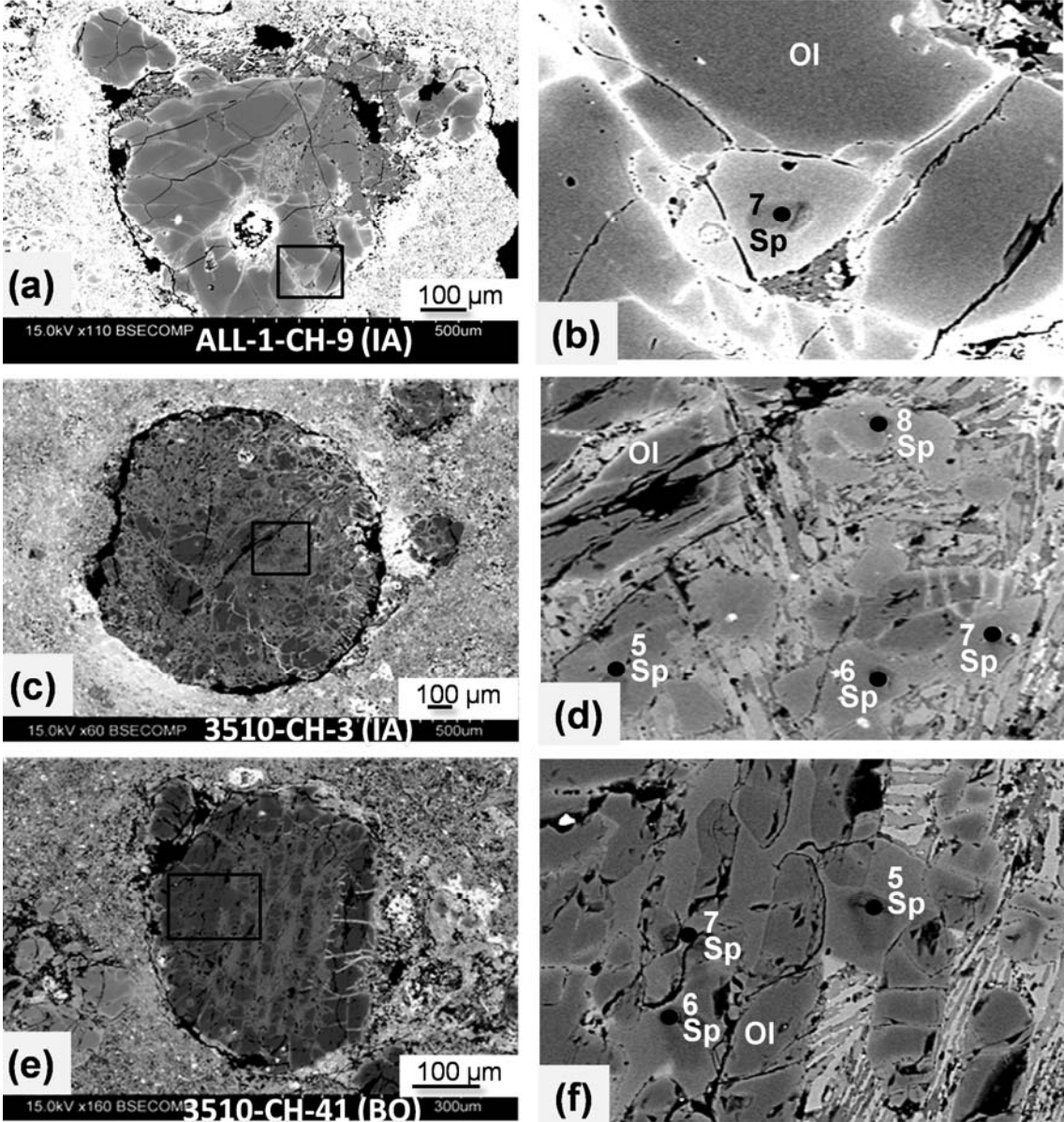


Fig. 12

